Turun yliopisto
University of Turku

HSD17B12 – AN ENZYME WITH A ROLE IN EMBRYONIC DEVELOPMENT, NORMAL OVARIAN FUNCTION AND CANCER

Heidi Kemiläinen (née Lagerbohm)

TURUN YLIOPISTON JULKAISUJA – ANNALES UNIVERSITATIS TURKUENSIS
Sarja - ser. D osa - tom. 1332 | Medica - Odontologica | Turku 2018

Turun yliopisto
University of Turku

HSD17B12 – AN ENZYME WITH A ROLE IN EMBRYONIC DEVELOPMENT, NORMAL OVARIAN FUNCTION AND CANCER

Heidi Kemiläinen (née Lagerbohm)

TURUN YLIOPISTON JULKAISUJA – ANNALES UNIVERSITATIS TURKUENSIS
Sarja - ser. D osa - tom. 1332 | Medica - Odontologica | Turku 2018

University of Turku

Faculty of Medicine

Institute of Biomedicine

Physiology

Turku Doctoral Programme of Molecular Medicine (TuDMM)

Research Centre for Integrative Physiology and Pharmacology

Supervised by

Professor Matti Poutanen
Institute of Biomedicine
Research Centre for Integrative Physiology and Pharmacology
University of Turku
Turku, Finland

Docent Leena Strauss
Institute of Biomedicine
Research Centre for Integrative Physiology and Pharmacology
University of Turku
Turku, Finland

Reviewed by

Professor Juha Tapanainen
Clinicum Helsinki
Department of Obstetrics and Gynecology
University of Helsinki
Helsinki, Finland

Assistant Professor Andrea Romano
Obstetrie & Gyneacologie,
School for Oncology and Develop Biol,
Fac. Health, Medicine and Life Sciences
University of Maastricht,
Maastricht, Netherlands

Opponent

Docent Tuuri Timo
Biomedicum Helsinki,
Program of Developmental and Reproductive Biology,
University of Helsinki
Helsinki, Finland

ISBN 978-951-29-7109-1 (PRINT)
ISBN 978-951-29-7110-7 (PDF)
ISSN 0355-9483 (Print)
ISSN 2343-3213 (Online)
Painosalama Oy – Turku, Finland 2018

To my family

"It is the time you have wasted for your rose
that makes your rose so important."

Antoine de Saint-Exupéry,
The Little Prince

ABSTRACT

Heidi Kemiläinen

HSD17B12 – An enzyme with a role in embryonic development, normal ovarian function and cancer

University of Turku, Faculty of Medicine, Institute of Biomedicine, Research Centre for Integrative Physiology and Pharmacology, In Turku Doctoral Programme of Molecular Medicine (*TuDMM*), Turku, Finland

Turku, 2017

At present, 14 different types of the hydroxysteroid (17-beta) dehydrogenase (HSD17B) enzymes have been characterized. These enzymes differ from each other according to tissue distribution, substrate specificity, subcellular localization and expression regulation. In this study, the main focus was to characterize the physiological function of one member of the enzyme superfamily, namely, hydroxysteroid (17-beta) dehydrogenase 12 (HSD17B12). HSD17B12 is widely expressed in different human tissues and has been suggested to function in fatty acid elongation as well as in sex steroid metabolism. However, the main function of HSD17B12 *in vivo* is still poorly understood.

The main aim of this study was to characterize the role of HSD17B12 in the ovarian physiology and fetal development. The HSD17B12 enzyme has a similar tissue distribution in mice and humans, and therefore, the HSD17B12 knockout mouse model was used to provide information about its role in humans. Furthermore, the expression of HSD17B12 enzyme was studied in different human epithelial ovarian cancer types.

According to our study, absence of the enzyme causes embryonic lethality, and even the loss of one allele leads to ovarian dysfunction and fertility problems in mice. Furthermore, we found that the expression of the HSD17B12 enzyme positively correlates with the grade of human ovarian cancer. However, the role of the enzyme in cancer progression is still poorly understood, necessitating further studies. In conclusion, our study indicates that the HSD17B12 enzyme is necessary for embryonal development and female fertility; however, its overexpression may play a role in ovarian cancer development and/or progression.

Keywords: *HSD17B12, ovarian function, embryonal development, ovarian cancer, fatty acids, prostaglandins*

TIIVISTELMÄ

Heidi Kemiläinen

HSD17B12 – tärkeä entsyymi alkion kehityksessä ja munasarjojen normaalissa toiminnassa sekä munasarjasyövässä

Turun yliopisto, Lääketieteellinen tiedekunta, Biolääketieteen laitos, Integratiivisen fysiologian ja farmakologian tutkimusyksikkö, Molekyylilääketieteen tohtoriohjelma (TuBS/TuDMM), Turku, Suomi

Turku, 2017

Hydroksisteroidi 17-beeta dehydrogenaasi (HSD17B) -entsyymit muodostavat ryhmän entsyymejä, joita on tällä hetkellä tunnistettu ihmisellä 14. Tässä tutkimuksessa on keskitytty hydroksisteroidi 17-beeta dehydrogenaasi 12 (HSD17B12) -entsyymin toiminnan tarkempaan selvittämiseen. HSD17B12 -entsyymi imenee laajalti ihmisen eri kudoksissa. HSD17B12:n ajateltiin aluksi olevan keskeisesti mukana steroidihormonien metaboliassa. Entsyymin on kuitenkin todettu osallistuvan myös rasvahappojen muodostukseen, erityisesti pitkien rasvahappojen elongaatioon. Siten HSD17B12-entsyymin kaikkia fysiologisia tehtäviä ei vielä varmuudella tiedetä.

Tämän tutkimuksen tarkoituksena oli selvittää HSD17B12-entsyymin fysiologinen tehtävä munasarjojen toiminnassa ja alkion kehityksen aikana käyttäen hiirimallia, josta on poistettu HSD17B12-geeni. HSD17B12-entsyymin kudosjakaumat ovat ihmisellä ja hiirellä hyvin samankaltaiset, joten selvittämällä entsyymin fysiologista merkitystä hiiressä, voi saaduista tuloksista tehdä johtopäätöksiä entsyymin merkityksestä myös ihmiselle. Lisäksi tutkimme HSD17B12:n ilmentymistä erilaisissa ihmisen munasarjasyövissä.

Tutkimustemme mukaan HSD17B12:n totaalinen puuttuminen häiritsee merkittävästi hiirten alkionkehitystä ja jo osittainen puutos aiheuttaa merkittäviä ongelmia naarashiirten hedelmällisyydelle. Lisäksi viimeisimpien tutkimustemme mukaan ihmisellä HSD17B12-entsyymin ilmentyminen korreloi munasarjasyövän pahanlaatuisuusasteeseen (gradukseen). Tämän osalta tutkimustiedot ovat kuitenkin vielä vähäiset ja jatkotutkimukset ovat tarpeen. Tutkimuksemme siten osoittavat, että HSD17B12-entsyymi on tarpeellinen alkionkehitykselle ja naaraan hedelmällisyydelle, mutta toisaalta sen liiallinen tuotto voi aiheuttaa munasarjasyöpää ja/tai sen progressiota.

Avainsanat: *HSD17B12, munasarjat, alkionkehitys, munasarjasyöpä, rasvahapot, prostaglandiinit*

TABLE OF CONTENTS

ABBREVIATIONS

AA	Arachidonic acid
Acetyl-CoA	Acetyl- coenzyme A
AKT	Thymoma viral proto-oncogene
ALA	Alpha-linolenic acid
5-ALOX	Arachidonate *5*-lipoxygenase
12-ALOX	Arachidonate 12-lipoxygenase
15-ALOX	Arachidonate 15-lipoxygenase
AMH	Anti-Müllerian hormone
AMHKO	Anti-Müllerian hormone knock-out mouse model
AREG	Amphiregulin
BMP15	Bone morphogenic protein 15
BMPs	Bone morphogenic factors
cAMP	Cyclic adenosine monophosphate
cGMP	Cyclic guanosine monophosphate
COX/PTGS	Cyclooxygenase/ Prostaglandin-endoperoxide synthase
COX 1	Cyclooxygenase 1
COX 2	Cyclooxygenase 2
COX 3	Cyclooxygenase 3
CYP450	Cytochrome P450
DAG	Diacyl glyceron
DHEA	Dehydroepiandrosterone
E	Embryonic day
E1	Estrone
E2	Estradiol
EET	Epoxyeicosatrienoic acid
EFA	Essential fatty acid
EGF	Epidermal growth factor
ELOVL	Elongation of very long chain fatty acid
$ELOVL_{1-6}$	Elongation of very long chain fatty acid 1-6
EP_2	Prostaglandin EP2 receptor
EP_{1-4}	Prostaglandin E_{1-4} receptor
Epi	Epiblast
ER	Endoplasmic reticulum
ERβ	Estrogen receptor β

EREG	Epiregulin
ERK1/2	Extracellular signal-regulated protein kinases 1 and 2
FA	Fatty acid
FAS	Fatty acid synthase
FOXO3a	Forkhead box O3A Phosphatase and tensin homolog
FP_{A-B}	Prostaglandin F_{A-B} receptor
FSH	Follicle stimulating hormone
GDF9	Growth differentiation factor 9
GDFs	Growth differentiation factors
GH	Growth hormone
GJA1	Gap junction 1 (Connexin-43)
GJA4	Gap junction 4 (Connexin-37)
GnRH	Gonadotropin-releasing hormone
GPR3	G-protein coupled receptor 3
HETE	Hydroxyeicosatetraenoic acid
5-HETE	5-hydroxyeicosatetraenoic acid
HSD17B	Hydroxysteroid (17-beta) dehydrogenase
HSD17B1	Hydroxysteroid (17-beta) dehydrogenase 1
HSD17B7	Hydroxysteroid (17-beta) dehydrogenase 7
HSD17B12	Hydroxysteroid (17-beta) dehydrogenase 12
ICM	Inner cell mass
IGF-1	Insulin-like growth factor 1
IP_3	Inositol triphosphate
IP-receptor	Prostacyclin/ prostaglandin I receptor
KAR	3-ketoacyl-CoA reductase
Kiss1	KISS-1 metastasis suppressor
LA	Linoleic acid
LH	Luteinizing hormone
LLC	Large luteal cell
LOX	Lipoxygenase
Malonyl-CoA	Malonyl-coenzyme A
MMP-2	Matrix metalloproteinase 2
MMP-9	Matrix metalloproteinase 9

NADPH	Nicotinamide adenine dinucleotide phosphate
NPPC	Natriuretic peptide C
NPR2	Natriuretic peptide receptor 2
P_4	Progesterone
PDE 3A	Phosphodiesterase 3A
PDE 5	Phosphodiesterase 5
PGs	Prostaglandins
PGE_2	Prostaglandin E_2
PGF2α	Prostaglandin F2α
PGDH	Hydroxyprostaglandin dehydrogenase
PGH_2	Prostaglandin H2
PGI_2	Prostaglandin I2
PGS	Primordial germ cell
PI3K	Phosphoinositide 3-kinase
PKA	Protein kinase A
PKC	Protein kinase C
Pla_2	Phospholipase A2
PLC	Phospholipase C
PND	Postnatal day
PR	Progesterone receptor
PrE	Primitive endoderm
PRL	Prolactin
Pten	Phosphatase and tensin homolog
PUFA	Polyunsaturated fatty acids
SER	Smooth endoplasmic reticulum
SLC	Small luteal cell
T	Testosterone
TE	Trophectoderm
TER	Trans-2,3-enoyl-CoA
TGF-β	Transforming growth factor beta
TP-receptor	Thromboxane receptor
TX	Thromboxane
VEGF	Vascular endothelial growth factor
VLFA	Very long fatty acids
WT	Wild type

LIST OF ORIGINAL PUBLICATIONS

This thesis is based on the following original publications, which are referred to in the by Roman numerals I – III:

I. Rantakari P,* **Lagerbohm H,*** Kaimainen M, Suomela J-P, Strauss L, Sainio K, Pakarinen P, and Poutanen M (2010)
Hydroxysteroid (17β) Dehydrogenase 12 Is Essential for Mouse Organogenesis and Embryonic Survival, Endocrinology, April 2010, 151(4):1893–1901
*P.R. and H.L. contributed equally to this work.

II. **Kemiläinen H**, Adam M, Mäki-Jouppila J, Damdimopoulou P, Damdimopoulos A.E., Kere J, Hovatta O, Laajala T.D., Aittokallio T, Adamski J, Ryberg H, Ohlsson C, Strauss L, Poutanen M (2016)
The hydroxysteroid (17β) dehydrogenase family gene HSD17B12 is involved in the prostaglandin synthesis pathway, the ovarian function, and regulation of fertility, Endocrinology (2016) 157 (10): 3719-3730.

III. **Kemiläinen H**, Huhtinen K, Carpén O, Strauss L, Poutanen M (2017)
The expression of HSD17B12 is associated with COX2 expression, and is increased in high grade epithelial ovarian cancer *(In press)*

1 INTRODUCTION

Hydroxysteroid (17-beta) dehydrogenases (HSD17Bs) catalyze the conversion between 17-keto and 17β-hydroxysteroids. Thus, the enzymes regulate the balance between biologically highly active and less active sex steroids, and they are considered to have an important role in regulating the ligand availability in various sex steroid-dependent tissues. HSD17B enzymes belong to two families: aldo-keto reductases and short-chain dehydrogenases/reductases. To date, in these two enzyme families, 14 different enzymes with HSD17B activity have been characterized. The enzymes possess different substrate and cofactor specificities, different tissue distributions, and different preferences for the direction of the reaction.

Mammalian hydroxysteroid (17-beta) dehydrogenase type 12 (HSD17B12) was initially characterized as a 3-ketoacyl-CoA reductase (KAR) involved in the long-chain fatty acid synthesis in endoplasmic reticulum (ER). In addition to its role in fatty acid (FA) synthesis, human HSD17B12 has been shown to catalyze the reduction of estrone (E1) to estradiol (E2) in HEK293 cells. In humans, the highest level of HSD17B12 has been detected in tissues involved in lipid metabolism, such as the liver, kidney and muscle, whereas in mouse, expression has also been detected in brown and white adipose tissues. Accordingly, recent studies *in vitro* have indicated that the enzyme participates in fatty acyl-CoA elongation by catalyzing the elongation of very long chain fatty acids (ELOVLs), particularly essential fatty acids (EFAs), such as arachidonic acid (AA).

AA and its downstream metabolites, which are called eicosanoids, are known to be involved in many biological processes, such as the regulation of female reproduction and embryonic development. However, eicosanoids have been linked to the development and progression of cancer. For example, there is strong evidence that AA and its downstream eicosanoids have a role in ovarian carcinogenesis. AA is metabolized by three main types of enzymes: cyclo-oxygenases (COXs), lipoxygenases (LOXs) and cytochrome P450 enzymes (CYP450s). The COX pathway produces prostaglandins (PGs), prostacyclins, thromboxanes (TXs) and hydroxy fatty acids, whereas the LOX pathway is responsible for the formation of leukotrienes, lipoxins and hepoxins. The CYP450 pathway forms epoxyeicosatrienoic acid (EET) and hydroxy fatty acids.

According to knowledge of the potential functions of the HSD17B12 enzyme and its assumed importance in the FA synthesis and steroid hormone metabolism, a genetically modified mouse line was generated for further studies. The mouse

model and human tissue samples were used to characterize the main function of the HSD17B12 enzyme in embryogenesis, female reproduction and ovarian cancer.

2 REVIEW OF THE LITERATURE

2.1 Ovarian function

2.1.1 *Estrous/menstrual cycle*

In mammals, the function of the ovaries is controlled by hormonal changes in estrous (rodents) or the menstrual (human) cycle. The length of the cycle varies among different species. In humans, the menstrual cycle is divided into two menstrual phases, follicular and luteal phases, and the average cycle length is 28 days (Sherman and Korenman 1975, Fehring, Schneider and Raviele 2006). The rodent estrous cycle is normally four to five days long and contains four different phases: proestrous, estrous, metestrous and diestrous. In mice, both ovaries go through the same morphological changes during the cycle, and ovulation occurs at the same time, bilaterally, releasing approximately 10-14 oocytes altogether.

In proestrus, follicles are developing rapidly until ovulation and estrogen levels start to elevate. Increasing estrogen levels are thought to signal and induce the surge of LH. The surge of LH and PRL induces estrous and starts ovulation and the ovulated follicles transform to the *corpus luteum* by luteinization, a remodelling process in which granulosa and theca cells are dramatically changed morphologically and biochemically. An ovulatory stimulus induces the changes and leads to the formation of luteal cells, and the proliferating activity of the cells starts to fade as the *corpus luteum* maturates (Sato, Nasu and Tsuchitani 2016). The *corpus luteum* starts to regress at metestrous and continues to regress in diestrous (luteolysis). The fading activity and regression of the *corpora lutea* leads to a new cycle of development and regression (Figure 1).

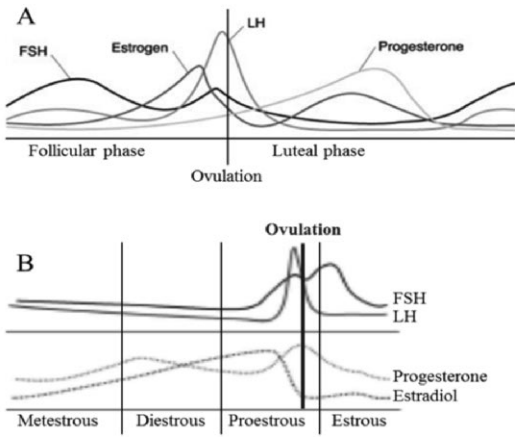

Figure 1. Hormonal change during (A) the human menstrual cycle and (B) the mouse estrous cycle
A - Modified from http://www. goldiesroom.org/ B - Modified from Miller et al 2014

Feedback effect of hormonal changes during the menstrual cycle regulates the cycle (Miller and Takahashi 2013) (Figure 2). LH stays low by negative feedback caused by estrogen. Before ovulation, the feedback of estrogen becomes positive, initiating the LH surge, after which the estrogen level rapidly decreases. During the luteal phase, LH and FSH levels decrease due to the rising levels of estrogen and P4, and without fertilization the hormonal cycle starts again (Levine et al. 1991).

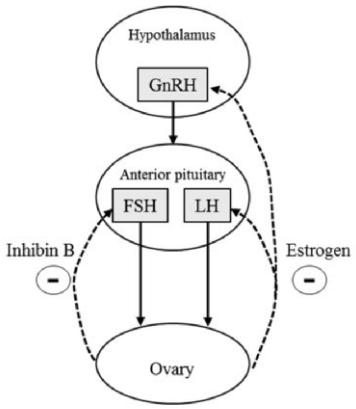

Figure 2. Regulatory feedback of hormonal changes during the estrous cycle. LH regulates hormone production of the theca and granulosa cells, and FSH regulates granulosa cell steroidogenesis. LH stimulates androgen production by theca cells. Androgens are transferred to the granulosa cells, where aromatase converts androgens to estrogens. FSH regulates aromatase activity and thus regulates E2 production. Estrogens inhibit the production of GnRH and LH. Granulosa cells also produce inhibin B, which inhibits the production of FSH.

2.1.2 *Follicular development*

Mammalian oocytes originate from embryonic precursors called primordial germ cells (PGCs). These precursors are formed from cells originating from the endoderm of the yolk sac. In mice, PGSs migrate to the developing ovary, into the genital ridge around embryonic day (E) 10.5 – 11.5. In humans, PGSs are first detected at the wall of the yolk sac at gestation week 3-4, whereas migration to the gonadal area takes place at gestation week 4. After reaching the genital ridge, the cells are termed oogonias, which are clustered in gonads forming the germline cysts. The cells then extensively multiply in the next few of days through mitotic division (Skinner 2005, Bristol-Gould et al. 2006, Xu and Gridley 2013, Mamsen et al. 2012), thus forming clonal cell clusters. In mice, the first part of the oogonias enters meiosis at around E13.5 and in humans at 11-12 weeks of gestation. The first meiotic division is finally arrested in the first phase of prophase I just before birth (Grive et al. 2016, Pepling 2012).

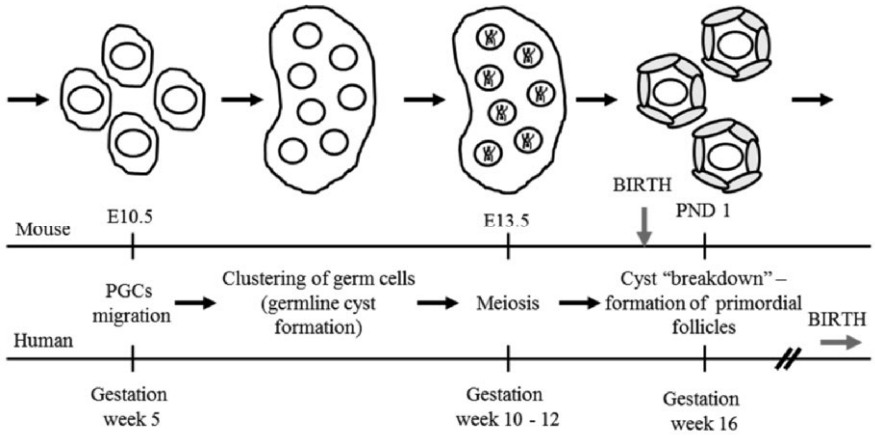

Figure 3. Development of primordial follicles. The main difference between mouse and human development is the timing of germline cyst breakdown. *Modified from Bristol-Gould et al 2006*

The cluster of germ cells, the germline cyst, starts to breakdown, and the oocytes are surrounded by somatic pre-granulosa cells. Although most of the oocytes are lost through apoptotic cell death, the surviving oocytes form the primordial follicles and thus the pool of the cells responsible for female fertility (Figure 3). The timing of germline cyst breakdown is species-specific; in mice, the cyst starts to breakdown after the first post-natal day, whereas in humans, cyst breakdown takes place approximately week 16 of gestation (Grive and Freiman 2015, Picton 2001).

The primordial follicles are formed when the single squamous layer of somatic cells (pre-granulosa cells) encircles the oocyte. The non-growing primordial follicles serve as the resource of developing follicles throughout the reproductive life of the female (Xu and Gridley 2013, Ding et al. 2010). The activation of primordial follicles is an irreversible process that ends either with fully grown preovulatory follicles and ovulation, or to atresia at some point of development. Due to the irreversibility of the process, it is important that the initiation and timing of activation is strictly controlled. The initiation of follicular growth is initiated by the change in shape of the granulosa cells from flattened to cuboidal, forming the primary follicle. Granulosa cells proliferate and increase in number, and the oocyte also expands in size (Monniaux 2016, Eppig 2001). When the granulosa cells form more than one layer around the oocyte, the follicle is called a secondary follicle. Although the follicular development of primary and secondary folli-

cles occurs without gonadotrophins, it is still highly sensitive to gonadotrophins, and optimal development to the preantral follicle requires these hormones (Pepling 2012) (Figure 4).

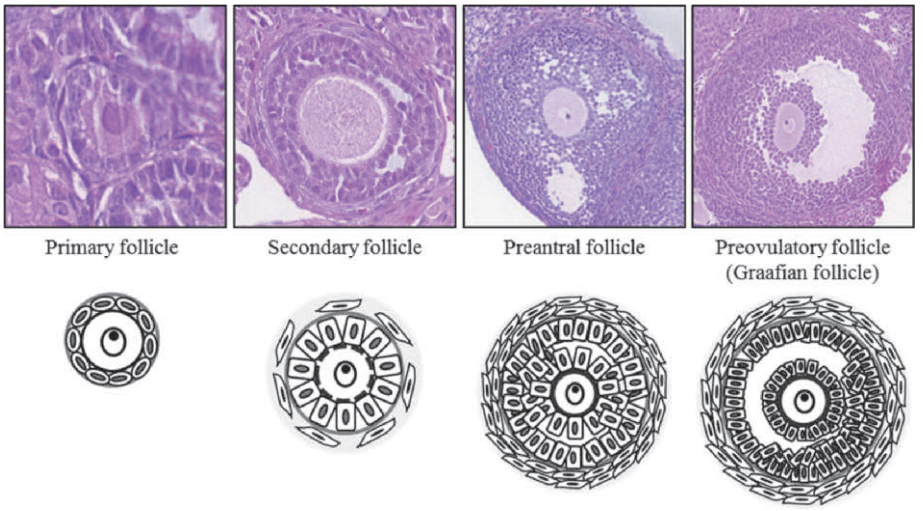

Figure 4. Histological chances in follicular development in mouse ovaries and schematic overview of follicle growth from the primordial to the preovulatory stage.

Secondary follicles are normally observed in mouse ovaries approximately 10-12 PND and in first preantral follicles at the age of 14-24 days (Matzuk et al. 2002). After antrum formation, the granulosa cells are divided into two different cell groups. Those near the oocyte are called cumulus cells, and those cells near the edge of the follicular wall are called mural granulosa cells. Although the granulosa cells express many common mRNAs and proteins, these two cell types have their own distinct expression profiles (Diaz, Wigglesworth and Eppig 2007). The development of secondary follicles (large preantral follicles) to antral follicles (tertiary follicles) occurs under FSH stimulation. During maturation, the mural cells start to produce increasing amount of estrogen which affect the hypothalamus, and the hypothalamus stimulates via GnRH the LH release from the pituitary. Cumulus cells support the growth and maturation of oocytes and participate in production. In addition, the cells are also involved in the production of the mucinous matrix of the antrum. During the LH surge, the cumulus cells start to expand and surround and separate the oocyte from the mural cells, leading to ovulation and release of the oocyte-cumulus cell complex into the oviduct (Kumar et al. 1997, Hussein, Thompson and Gilchrist 2006, Diaz et al. 2007).

Theca cells compose form the outer cell layer of the follicle. In primordial and primary follicles, there are no theca cells, but after the formation of the secondary follicle, the theca cell layer starts to develop from the stromal cells near the follicle in response to signalling from granulosa cells (Tajima et al. 2007). Theca cells form two different layers, theca interna is a highly vascularized layer of active steroidogenic cells immediately adjacent to the basal lamina, whereas the theca externa is a loosely organized layer of inactive steroidogenic cells localized between the interfollicular stroma and the theca interna (Magoffin 2005). The putative precursors of theca cells do not express the LH receptor. Thus, theca cell differentiation is gonadotrophin-independent (Young and McNeilly 2010). Consequently, it has been assumed that the development auto and paracrine signalling to follicle itself promotes the development of theca cells from the stroma. Although many studies have assessed the development of theca cells from the stroma, the specific factors has yet to be discovered.

2.1.3 *Molecular factors underlying folliculogenesis*

In humans and other mammals, the ovarian follicle is the core unit of the female reproductive system. In humans, naturally occurring mutations in genes encoding BMP ligands have been found to lead to severe problems in human reproduction (Chang, Qiao and Leung 2016). Although the fundamental process of follicular development is very similar within different species, most studies have utilized rodent models.

2.1.3.1 PI3K/AKT pathway and follicular maturation

Oocyte quality is the main limiting factor in female fertility. Oocytes are known to be regulated by the surrounding microenvironment. Oocytes and granulosa cells communicate via gap junctions, including three different surrounding connexins: 32, 43 and 45 (Richard and Baltz 2014, Ackert et al. 2001).

Although the molecular mechanism of selection of proliferating primordial follicles is not clearly known, oocytes play an important role in the development of follicles after the primordial stage. Mouse studies have shown that the activity of the PI3K/AKT pathway in oocytes place a central role in the initiation of primordial follicle differentiation (Brown et al. 2010, Liu et al. 2006). PI3K activates AKT, leading to the hypermethylation of FOXO3a and nuclear export, which allows the primordial follicles to evolve to primary follicle and further mature and to further mature. The FOXO3a knockout mouse model initially showed

normal initiation of follicle development and ovulation (Castrillon et al. 2003). However, the development of the primordial follicles was uncontrolled, eventually leading to a lack of primordial follicles. Females first produce larger litters, but as early as 15 weeks of age, all the follicles are depleted, causing total follicular atresia and secondary infertility. To study further the mechanism of FOXO3a in the initiation of follicular development, the role of *Pten* in the process was studied (John et al. 2008). *Pten* is known to act as a gatekeeper in the PI3K/AKT pathway, and as expected, oocyte-specific ablation of *Pten* leads to hyperactivity of AKT and increased phosphorylation of FOXO3a, consequently leading to premature follicular demise and to infertility (John et al. 2007, John et al. 2008, Uhlenhaut and Treier 2011, Makker, Goel and Mahdi 2014). *Reddy et al* studied an oocyte specifically deleted Pten mouse model and reported results consistent with those obtained for FOXO3a, further validating the mechanism of premature follicular maturation. Interestingly, elevated serum levels of LH and FSH have also been observed in mice with a genome-specific deletion of Pten (Reddy et al. 2008).

2.1.3.2 GDF9 and BMP15 control early folliculogenesis

Mouse studies have also shown that *GDF9* (growth differentiation factor 9) and *BMP15* (bone morphogenetic protein 15) are both secreted by oocytes and both function in granulosa cells, further supporting the differentiation of granulosa cells. GDF9 knockout female mice are infertile as a consequence of a total block in folliculogenesis at the primary follicle stage. In addition, *in vitro* studies have shown that *GDF9* regulates cumulus cell expansion and hyaluronan synthase 2, COX-2, EP2 and LH receptor activities (Joyce et al. 2000, Yan et al. 2001, Kidder and Vanderhyden 2010, Otsuka, McTavish and Shimasaki 2011). BMP15 knockout female mice are subfertile mainly as a consequence of the defects in ovulation and early embryonal development. The double knockout mouse model of *GDF9* and *BMP15* is also infertile, mimicking the GDF9 knockout mouse. These double knockout mice show loss of oocytes and germline cysts and also an arrest at the primary follicle stage (Yan et al. 2001, Su et al. 2004).

In contrast, sheep carrying a *BMP15* deletion are infertile. Follicular development is arrested at the primary/secondary follicle stage, and none of the follicles develop further. Moore and co-workers showed that ewes with *BMP15* point mutations in both alleles had similar fertility problems as *GDF9* knockout mice, which can be explained by *in vitro* studies showing that the mutated BMP15 inhibits GDF9 secretion (Moore, Erickson and Shimasaki 2004).

2.1.3.3 Anti-Müllerian hormone in folliculogenesis

Anti-Müllerian hormone (AMH) expression is first detected in early primary follicles, with the highest expression detected in granulosa cells of the pre-antral and small antral follicles. However, AMH expression is not detected in primordial follicles, theca cells and oocytes or in the ovarian stroma. The distribution of AMH expression varies inside the follicle so that the expression levels are highest in the granulosa cells surrounding the antrum and oocyte. In addition, the AMH expression varies between the follicles, with those undergoing atresia showing elevated AMH expression, in contrast to a complete loss of expression during formation of the *corpus luteum* (Durlinger et al. 1999, Durlinger et al. 2002).

The knockout of AMH does not affect to fertility of female mice and ovaries do not show defect. Surprisingly, the loss of AMH did not affect the fertility of the female mice and the ovaries did not show any major defects. In the absence of AMH, a larger population of primordial follicles developed into primary or secondary follicles at an earlier age of compared with WT females. As a consequence of earlier activation of primordial follicle, the AMHKO females had fewer primordial follicles than WT females later in life (Behringer, Finegold and Cate 1994, Durlinger et al. 1999).

2.1.4 *Control of meiosis in oocytes*

In mitosis, cells form two identical daughter cells, so called diploid cells with replicated chromosomes, whereas in meiosis, the genetic information is divided into haploid cells. In meiosis, there are two division phases, meiosis I and meiosis II. During meiosis I, the homologous chromosomes are separated to opposite poles, and in meiosis II the sister chromatids are separated. Thus, in meiosis II, non-identical haploid gametes are formed (Marston and Amon 2004).

In the follicle, the oocyte is surrounded by somatic granulosa cells and extracellular matrix (Eppig, Wigglesworth and Pendola 2002). During follicle growth, the meiotic division of oocytes is arrested in prophase I, and it is well-established that the arrest in prophase is dependent on high levels of cAMP inside the oocyte (Handel and Schimenti 2010).

Regulation of the cAMP concentration and meiotic arrest are based on bilateral communication between oocytes and granulosa cells. This communication occurs through the follicular fluid and gap junctions. Two vital isoforms of gap junc-

tions have been identified and localized in the maturating follicle: GJA1 (connexin-43) and GJA4 (connexin-37). Connexin-43 is localized between the granulosa cells and connexin-37 in the zona pellucida, providing an information gate between oocytes and granulosa cells (Richard and Baltz 2014). Normal function of gap junctions is needed for the maintenance of prophase I. During ovulation, the LH peak affects the gap junctions, leading to the resumption of meiosis (Conti et al. 2002, Conti et al. 2012). A knockout mouse model for connexin-37 showed that the protein is essential for female fertility (Simon et al. 1997). Lack of connexin-37 nearly completely prevented the formation of antral follicles and caused abnormal formation of the *corpora lutea*. Interestingly, females with one functional allele showed fewer gap junctions but were fertile and had normally developing follicles. This finding indicates that even partially functional gap junctions are sufficient to allow follicular development. Although the females clearly showed fertility problems, all the genetically modified male mice were fertile.

Recent studies have shown that the cGMP level in somatic cells plays an important role in maintaining the level of cAMP in the oocyte. Natriuretic peptide precursor C (NPPC) is released from mural granulosa cells and diffuses through the gap junctions to the antral fluid. It binds to the transmembrane guanylyl cyclase natriuretic peptide receptor 2 (NPR2), which is known to be expressed only in the cumulus granulosa cells and not in oocytes (Shuhaibar et al. 2015, Liu et al. 2013). The activation leads to the production of cGMP from granulosa cells by phosphodiesterase PDE5, and cGMP is transferred through granulosa cell gap junctions to the oocyte. In the oocyte, cGMP inhibits PDE3A and allows GPR3 G_S-linked G-protein coupled receptor (GPR3) to produce cAMP and maintain the meiotic arrest (Figure 5) (Vaccari et al. 2008, Vaccari et al. 2009).

During ovulation, the LH peak leads to the decrease in cAMP levels inside the oocyte and inactivates PDE5, which in turn decreases cGMP levels. Decreased cGMP levels lead to de-phosphorylation and activation of PDE3, and consequently, decreased cAMP levels inside the oocyte (Celik et al. 2015, Conti et al. 1998) (Figure 5).

Following the decrease in cAMP levels in the oocyte, the nucleus breaks down and spindle formation starts. The homologous chromosomes begin to separate, and half of them start to atrophy to a small compartment called the polar body. The remaining half of chromosomes stay arrested in the metaphase II spindle until the oocyte is fertilized (Duncan, Moss and Williams 2006). Although the LH surge starts the cascade that promotes meiosis via cAMP, prostaglandin E_2 (PGE_2) has also been shown to be involved in regulating cAMP levels downstream of the LH signal (Rich et al. 2007). Meiosis will be completed only when the oocyte undergoes ovulation and is fertilized (Downs 2010). Oogenesis is

strictly controlled, and any problems in these critical developmental windows may cause infertility, aneuploidy or miscarriage.

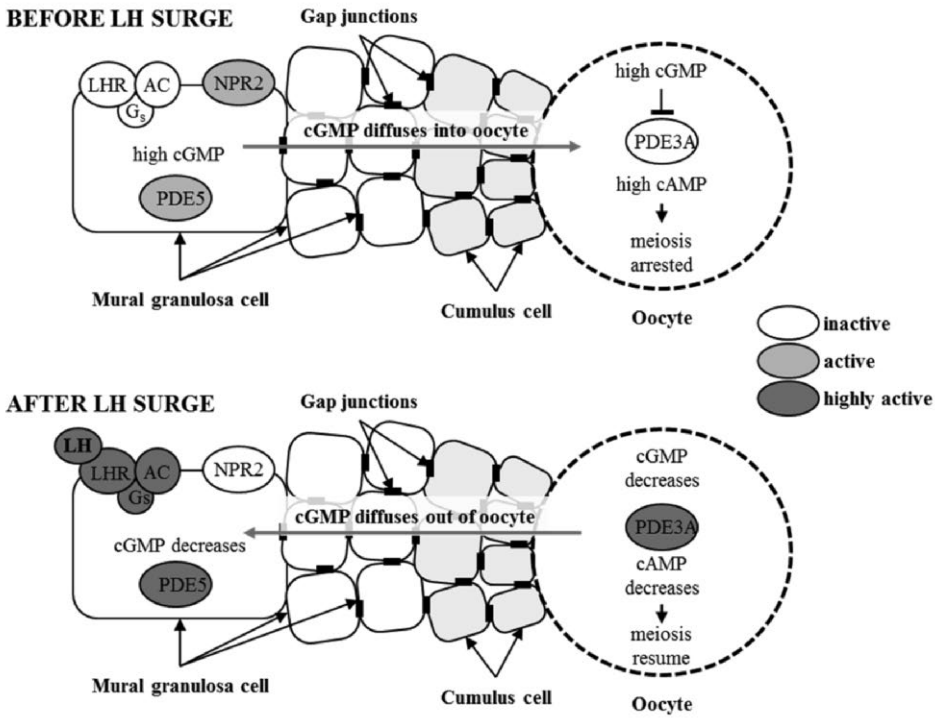

Figure 5. Control of oocyte meiotic arrest. Before the LH surge, NPR2 produces cGMP in mural granulosa cells, while PDE5 degrades cGMP such that the concentration of cGMP is maintained. cGMP diffuses through gap junctions to the oocyte and inhibits PDE3A, leading to high cAMP levels in the oocyte and arrested meiosis. The LH surge inhibits NPR2 and activates PDE5, leading to a significant decrease in cGMP levels in mural granulosa cells. cGMP starts to diffuse out of the oocyte, leading to activation of PDE3A, which in turn initiates the degradation of cAMP. Decreased cAMP levels lead to the resumption of oocyte meiosis. *Modified from Shuhaibar et al. 2015 and Downs et al. 2014.*

2.1.5 *Ovulation*

Ovulation is tightly controlled by FSH and LH (Kumar and Sait 2011). FSH stimulation is obligatory for developing follicles at the preovulatory stage (Raju

et al. 2013). In contrast, the LH surge rapidly initiates the final differentiation of mural granulosa cells and cumulus cells, leading to the resumption of meiosis and expansion of cumulus cells and eventually ovulation (Figure 6) (Hizaki et al. 1999). Mural granulosa cells start to luteinize and form the *corpus luteum* after ovulation. FSH and LH activate many complex pathways, for example, the cAMP/PKA, ERK 1/2 and PI3K/AKT pathways (Ben-Ami et al. 2006, Takahashi et al. 2006).

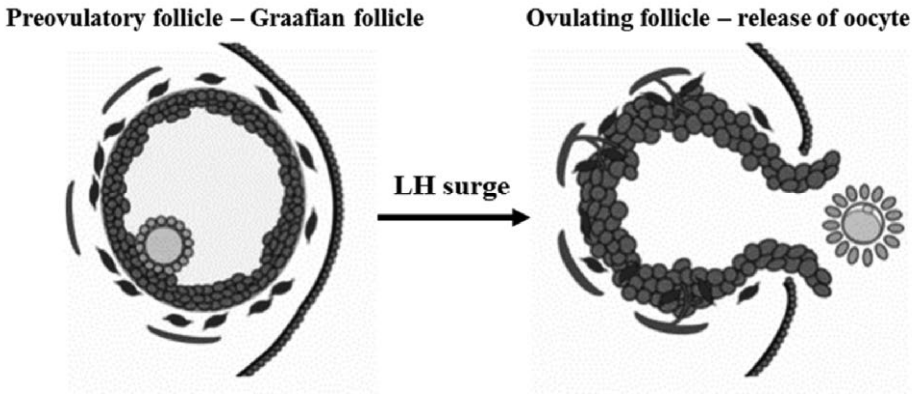

Figure 6. Schematic view of the release of an oocyte from the follicle**.**
Modified from Duffy M. D. 2015 Review

In rodents, the preovulatory LH surge is initiated by a dramatic increase in the level of E2 produced by the fully maturated preovulatory follicle (Wide and Eriksson 2013). The LH surge affects the theca and granulosa cells through the LH receptor. Interestingly, the LH receptor in rodents are not detected in cumulus cells during ovulation. In addition, LH is known to affect these cells indirectly. Amphiregulin (AREG), epiregulin (EREG) and betacellulin (BTC) are produced rapidly after the LH surge in granulosa cells, but possibly also in theca cells (Light and Hammes 2015). AREG and EREG mediate the LH signal to cumulus cells and the oocyte.

Nautiyal and co-workers (2010) showed that RIP140$^{-/-}$ (receptor-interacting protein 140) mice were infertile due to the presence of unruptured follicles and oocytes sequestered inside luteinizing follicles. Interestingly, RIP140$^{+/-}$ mice were also subfertile, and only half of the follicles were able to ovulate (Nautiyal et al. 2010). RIP140 has been suggested to regulate LH-induced expression of AREG, EREG and BTC, and RIP140$^{-/-}$ cumulus cells showed decreased expression of AREG *in vitro*. Shimada and co-workers (2006) showed that PTGS2 null mice

(also known as COX-2 null mice) expressed significantly lower levels of AREG and EREG, but not BTC, in cumulus cells *in vitro* compared with their WT controls. In addition, they showed *in vitro* that LH induced EGF-like factors via RIP140, which activated Ptgs2/COX-2 enzyme, thus leading to increased PGE_2 synthesis (Shimada et al. 2006).

Both EP1 and EP3 receptor knock-out mice were fertile and had no alterations in embryonic development (Ushikubi et al. 1998), whereas EP2-deficient mice showed significantly decreased fertility in females. EP2 null females delivered smaller litters and had a decreased ovulation rate because the oocytes remained trapped inside the *corpora lutea*. Most of the EP2 null follicles did not exhibit normal cumulus cell expansion before ovulation, causing fertilization problems. Interestingly, the phenotype of EP2-deficient females was similar to that of COX-2-deficient females (Hizaki et al. 1999, Kennedy et al. 1999, Tilley et al. 1999). Although EP4-deficient mice displayed normal embryonal development, the mice died quickly after birth, with the oldest surviving until the third postnatal day, as a consequence of lack of ductus arteriosus closure (Nguyen et al. 1997, Segi et al. 1998).

COX-1 deficient mice were found to be surprisingly healthy. Whereas COX-1 null males were fertile, females had difficulties in induction of parturition, and almost all pups were born dead or died shortly after birth. In contrast to the COX-1-deficient mice, COX-2-deficient mice had severe problems, and only half of the pups survived to weaning. COX-2-deficient females were infertile, showing alterations in cumulus cell activation. Furthermore, stigmata formation (the exact place were ovulation happens) and ovulation were abnormal (Lim et al. 1997, Langenbach et al. 1999).

LH induces the expression of progesterone receptor (PR) and COX-2, which leads to prostaglandin synthesis in the preovulatory follicles. PGs modulate proteolytic activity by activating proteolytic inhibitors and preventing the breakdown of the theca layers throughout the follicle wall (Gaytán et al. 2003). PR enables the apex and ovarian surface to break down and release the oocyte into the periovarian space. Elevation of the PGE_2 concentration is thought to control the timing of ovulation (Mikuni et al. 1998). The increased levels of PGE and F and also increased hydroxyeicosatetraenoic acid (HETE, see Figure 13) levels can be detected in follicular fluid just before ovulation (Sugimoto et al. 1997, Ochsner et al. 2003, Dozier, Watanabe and Duffy 2008). PGs induce proteolytic activities, and HETE induces angiogenesis and overall blood flow. In particular, PGE_2 induces proteolytic activity in follicles (Downey, Mootoo and Doyle 1998). The proteolytic enzymes digest collagens in the follicular wall, allowing the cu-

mulus-oocyte-complex to be released from the follicle. PGE_2 is also thought to activate the smooth muscle cells in the ovaries and thereby enhance ovulation (Takahashi et al. 2006, Duffy 2015).

During ovulation, follicular rupture needs to occur properly so that the oocyte is released in the right direction. If the effects of PGs are inhibited during ovulation, the oocyte remains trapped inside the follicle and ovulation does not occur (Gaytán et al. 2003). Gaytán and co-workers showed that blocking prostaglandin synthesis caused an incorrect direction of ovulation, or the oocytes were completely unable to ovulate. Therefore, it can be concluded that PGs are required for targeted follicle rupture and correct ovulation. Because of their ability to inhibit ovulation, PGs are also thought to be useful as emergency, but not monthly, contraceptives (Duffy 2015).

Interestingly, further studies by Gaytán and co-workers showed that although the administration of indomethacin did not reduce the mRNA level of COX2 but decreased PG levels, it significantly reduced *Kiss1* mRNA levels in rodent ovaries (Gaytán et al. 2009). Furthermore, *Kiss1* expression was rescued by the administration of PGE_2. Although Kiss1 is a well-known neuropeptide that regulates the release of GnRH from the brain during the hormonal cycle (Tomikawa et al. 2012), recent studies have shown that intraovarian Kiss1 also regulates follicular development (Fernandois et al. 2017).

2.1.6 *Luteinisation of corpora lutea*

During ovulation, the LH surge rapidly initiates the final differentiation of mural granulosa and theca cells. In most nonprimate mammals, granulosa cells form a pool of large luteal cells (LLCs) and theca cells form small luteal cells (SLCs) (Nelson et al. 1992, Arosh et al. 2004). LLCs and SLCs are heavily reorganized with fibroblasts and endothelial cells while forming the *corpus luteum.* In contrast, in primates, LLCs are called granulosa-lutein cells and SLCs are theca-luteal cells. In addition, the luteinized cells in primate ovaries are notably less reorganized, and the cells remain separated in the *corpus luteum*, unlike in nonprimate ovaries (Olofsson and Leung 1994, Niswender et al. 2000).

The preovulatory surge of LH affects the steroidogenic pathway so that P_4 becomes the primary hormone produced by the ovaries. P_4 is one regulator of the length of the reproductive cycle, and it is needed for the maintenance of pregnancy. Thus, dysfunctions in P_4 production have been linked to infertility, abortion and ovarian cycle disorders. In SLCs, LH also activates adenylate cyclase and

increases cAMP levels, leading to PKA activation in the cells. PKA increases the release of cholesterol from cholesterol esters, and cholesterol is in turn metabolized to P4 (Arosh et al. 2004).

Prostaglandin I_2 (PGI_2) and PGE_2 both act as luteotropic hormones in luteal cells, PGI2 in SLCs and PGE_2 in LLCs (Wiltbank, Belfiore and Niswender 1993). PGs are thought to function in the same manner as LH in luteal cells, thus increasing the cAMP level and activating protein kinase A (PKA), leading to the formation of P_4. PGI_2, PGE_2, GH and IGF-I all increase the synthesis of P_4 in LLCs (Wiltbank et al. 1990).

Once the *corpus luteum* has reached the mature size and maximum potential of P_4 secretion, it remains functional for a few of days, depending on the species. In the absence of pregnancy, the luteal cells start to regress, and the next reproductive cycle can start (Niswender et al. 2000).

2.1.7 *Luteolysis of corpora lutea*

Luteolysis means basically the decomposition of the *corpus luteum*. First, the luteal cells lose the ability to produce P4; second, they start to diminish themselves. In most mammals including rodents, prostaglandin $F_{2\alpha}$ ($PGF_{2\alpha}$) originating from the uterus is the main factor initiating luteolysis (Figure 7). $PGF_{2\alpha}$ is produced in the uterine horn and reaches the ipsilateral ovary via ovarian artery. In this way, it does not need to travel through the pulmonary circulation, where it would be inactivated (Olofsson and Leung 1994).

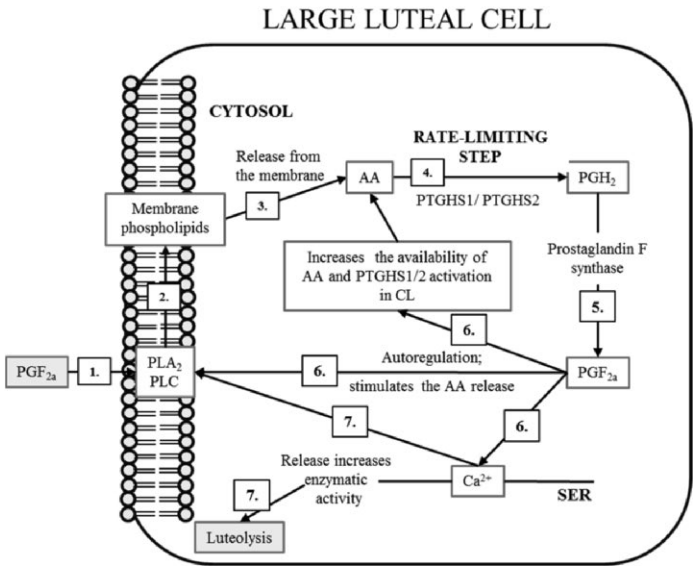

Figure 7. The role of PGs in the mechanism of luteolysis; in rodents, $PGF_{2\alpha}$ is first synthesized in the uterus and transferred to the ovary. $PGF_{2\alpha}$ starts the cycle that results in the release of Ca^{2+}, which in turn leads to luteolysis.

However, in primates and human ovaries, the luteal $PGF_{2\alpha}$ is produced in the ovaries and is locally affected. Thus, the release of $PGF_{2\alpha}$ affects the luteal cells in an autocrine and paracrine manner (Lee et al. 2010). $PGF_{2\alpha}$ affects the blood flow inside the *corpus luteum*. Decreased blood flow is one way to induce luteolysis, as the level of nutrients and cholesterol is reduced, leading to the inability to produce P4. $PGF_{2\alpha}$ activates membrane-bound phospholipase C (PLC), leading to increased intracellular IP_3 and DAG concentrations (Figure 8). Elevated levels of IP_3 increase the release of free Ca^{2+} from smooth endoplasmic reticulum (SER), which activates PKC (protein kinase C). Thus, PGs are thought to mediate PKC-induced apoptosis in LLCs (Juengel et al. 2000, Skarzynski, Ferreira-Dias and Okuda 2008).

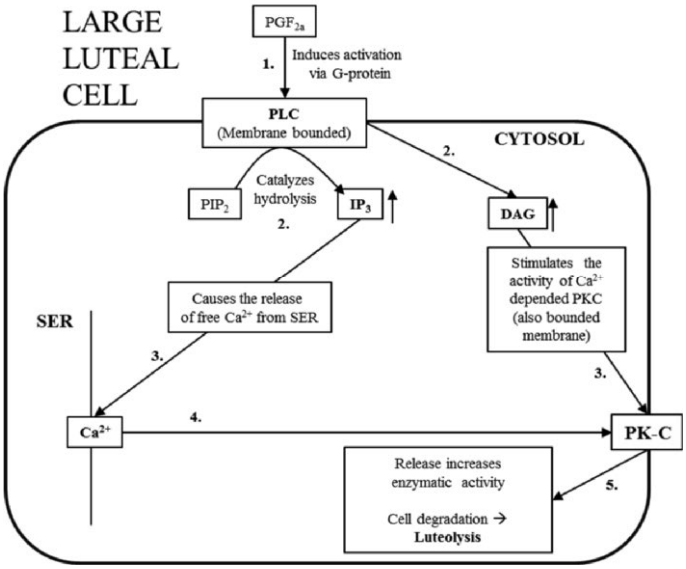

Figure 8. Signal transduction underlying the mechanism of luteolysis in LLCs.

PGE_2 and $PGF_{2\alpha}$ function via G-coupled receptors; PGE_2 is known to have four receptor subtypes ($EP_{1\text{-}4}$) and $PGF_{2\alpha}$ two receptor subtypes ($FP_{A\text{-}B}$)PGE_2 and (Narumiya, Sugimoto and Ushikubi 1999). During activation, EP_2 and EP_4 are coupled to adenylate cyclase and induce the production of cAMP, which in turn activates PKA. EP_1 and FP are coupled to PLC. PLC generates IP_3, which promotes the release of Ca^{2+} and diacylglycerol (DAG), and further activates protein kinase C (PKC). The functions of FP receptors in luteal tissues have been widely studied, whereas the functions of EP receptors in luteal tissues are still largely unknown (Arosh et al. 2004).

In the case of a pregnancy, the *corpus luteum* becomes resistant to $PGF_{2\alpha}$ - induced luteolysis. One way of preventing *corpus luteum* degradation is to increase the catabolism of $PGF_{2\alpha}$ (Sakamoto et al. 1995). The 15-

hydroxyprostaglandin dehydrogenase (PGDH), which is known to be the rate-limiting enzyme in inactivation of the PGE and F series, is widely expressed in almost all tissues, and the human chorion is known to express high levels of PGDH during early pregnancy, in this way shielding the cells from the effects of uterus-originating $PGF_{2\alpha}$ (Silva et al. 2000).

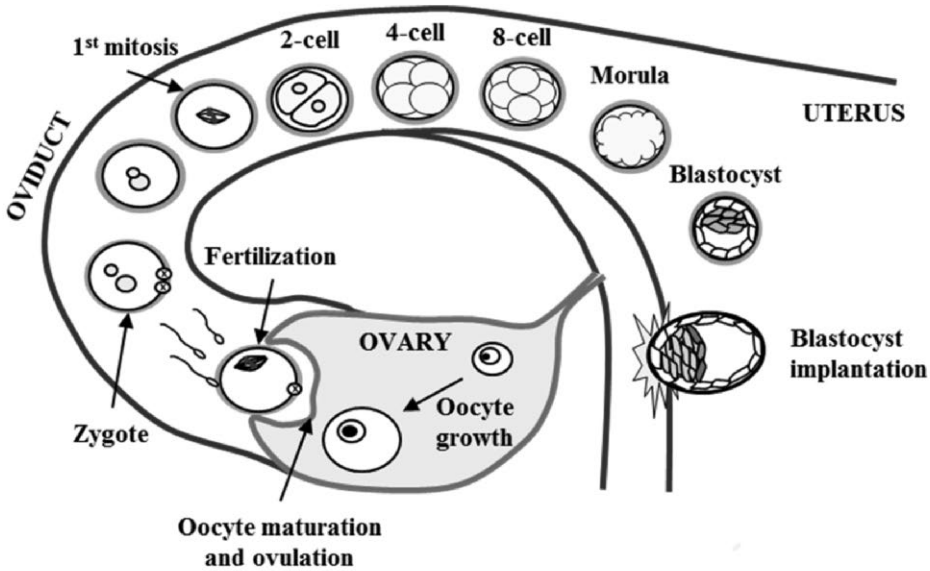

Figure 9. Ovulation, fertilization and implantation (human).
Modified from Dard et al. 2008 and Clift and Schuh 2013

2.2 Early embryo development – from zygote to organogenesis

2.2.1 *From zygote to blastocyst*

Embryonic development starts when the oocyte is fertilised (Figure 9). The fertilized oocyte is also called a zygote. This preimplantation period lasts approximately four days in mouse, and during this time the zygote develops into the implanting blastocyst (Artus and Cohen-Tannoudji 2008). In humans, the same development takes six to nine days. First, a dense cluster of cells are formed, and the zygote starts to divide with no significant growth in size, at the 8-cell stage, the blastomer start to show the first signs of polarity. Intercellular adhesion increases, leading to compaction and thus producing the morula. The polarity of the blastomer is important for normal formation of the inner cell mass (ICM) and

further formation of the embryo (Dard et al. 2008, Artus and Chazaud 2014). In the morula, the cells first aggregate very closely, but soon divide into two cell layers. The outer layer of cells forms the trophectoderm (TE), the main function of which is to form the embryonic part of the placenta, whereas the ICM develops into the embryo (Marikawa and Alarcón 2009). At the 32-cell stage, the TE layer develops into the fully functional epithelium. The cell layer contains functional Na^+/K^+ ATPases and aquaporins, thus allowing water and ions to accumulate inside the morula (Bell and Watson 2013). During the formation of the fluid-filled cavity (also known as the blastocoel), the morula slowly transforms into a blastocyst (Clift and Schuh 2013).

While the blastocyst is expanding, the TE layer is differentiating based on the close vicinity of the ICM, resulting in polarity of TE cells immediately adjacent to the ICM. At the time of implantation, the ICM has formed two cell lineages: epiblasts (Epi) and primitive endoderm (PrE) (Chazaud et al. 2006). Epi surrounds one and PrE surrounds the other side of the TE layer. PrE surrounds part of the blastocoel. Before implantation, the TE layer starts to hatch through the zona pellucida, permitting implantation into the uterus. In addition, implantation of the blastocyst into the decidualized endometrium consistently occurs via the polar TE portion (Gamage, Chamley and James 2016).

De novo FA synthesis is vital for normal embryonal development, as lipids are needed for the formation of cell membranes. A knockout mouse model of fatty acid synthases (FAS) was shown to be embryonic lethal, demonstrating the importance of FA synthesis in embryos development. $FAS^{-/-}$ embryos died prior to implantation, and some $FAS^{+/-}$ embryos died during various stages of embryonic development. At embryonic day 9.5, $FAS^{+/-}$ showed retarded development; the embryos did not finish turning, and they were significantly smaller than the WT littermates (Chirala et al. 2003).

2.2.2 *Gastrulation*

In gastrulation, the ICM is reorganized into a three-layered structure. These three layers are termed the ectoderm, mesoderm and endoderm. After the differentiation of trophoblasts, a layer of the ICM starts to flatten (forming the so-called embryonic disk), forming a small internal sac called the amniotic cavity. The floor of the amniotic cavity is formed by the embryonic ectoderm (Boroviak and Nichols 2017). After formation, the embryonic disk starts to transform in shape, and one end starts to widen. The narrow (posterior) end is called the primitive streak (formed from ectoderm), and the anterior end is termed the primitive node,

the end of which forms a knob-like thickening. The primitive groove forms on the surface of the streak, which looks like a shallow groove in the surface (Figure 10). From the side of the primitive streak is a third cell layer, the mesoderm, which is between the ectoderm and endoderm layers. All three cell layers have their own specific characteristics and give rise to different tissues of the body (Downs 2002).

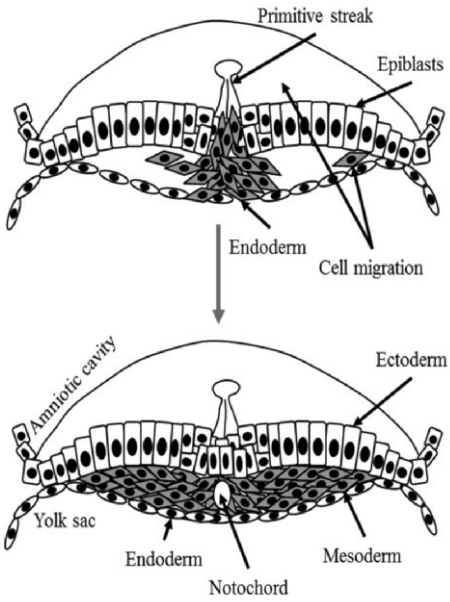

Figure 10. Gastrulation – formation of three germ cell layers. The Epi layer starts to fold and form a shallow groove. Endoderm cells migrate and differentiate into endoderm and mesoderm layers.
Modified from classes.midlandstech.edu/ carterp/ Courses/ bio211/ chapter28/ chap28.htm

PGE_2 is essential for cell migration during gastrulation. Although COX-1 null mice were relatively normal, studies conducted using zebrafish embryos showed a significant role of COX-1, but not COX-2, in prostaglandin metabolism during gastrulation, and COX-1 expression co-localized with cytosolic PGE_2 synthase (Cha et al. 2006). Cha and co-workers also showed that COX-2 expression was detectable until the end of gastrulation.

2.2.3 *Formation of the early nervous system*

In front of the streak, two longitudinal ridges are formed by folding up of the ectoderm. These ridges are called neural folds, between which lies a shallow neural groove. While the neural folds are elevated, the groove slowly deepens and finally forms a closed tube, the neural tube (Ezin, Fraser and Bronner-Fraser 2009). The fusion of the neural folds occurs first at the zone where the hind brain will form. Before the neural groove is completely closed, the ectodermal cells migrate

along the ridge of the neural folds. These cells form a basement for the sympathetic nervous system, and thus the cells form the so-called neural crest or ganglion ridge (Theveneau and Mayor 2010). While the mesoderm is growing over the neural tube, the overlying layer of ectodermal cells become separated from the neural tube (Theveneau and Mayor 2012).

In the cephalic end of the neural tube, three primary cerebral vehicles form after a series of dilatations. These three structures are the future brain segments: forebrain, midbrain and hindbrain. The walls of the vehicles form the nervous tissue and neuroglia, while the cavities form the ventricles of the brain. The rest of the tube forms the spinal cord, and the cavity remains as the neural canal (Creuzet, Martinez and Le Douarin 2006).

Closure of mammalian neural tube is known to require more than 100 genes functioning in a correct manner, including Pten. Pten null mice are embryonic lethal, and mouse embryos die around embryonic day 7.5 (Di Cristofano et al. 1998, Yeh et al. 2011). Thus, they show a severe defect in neural plate formation and closure. Lack of PTEN leads to the loss of cell polarity, causing problems in cell migration along the apical-basal axis and the failure of cells to form the columnar neural epithelium. Therefore, PTEN is suggested to be required for stabilization of cell packing during the formation of neural plates (Bloomekatz et al. 2012, Grego-Bessa et al. 2016).

2.3 Hydroxysteroid (17-beta) dehydrogenase enzymes

In humans, 14 different types of HSD17B enzymes have been characterized to date. These enzymes differ from each other by their tissue distribution, substrate specificity, subcellular localization and regulation. HSD17Bs catalyze the conversion between 17-keto and 17beta-hydroxysteroids. Among the sex steroids, the 17beta-hydroxy forms are the highly active forms, whereas the corresponding 17-keto forms are biologically less active. Several HSD17Bs may also metabolize other substrates, such as alcohols, bile acids, FAs and retinols (Adamski and Jakob 2001, Mindnich, Möller and Adamski 2004, Saloniemi et al. 2012)

Table 1 Different human HSD17B enzymes and their main enzymatic function. Data collected form http://www.genecards.org/ (human gene database).

Enzyme	Biological functions	Enzymatic reaction
HSD17B1	Steroid metabolism	Estrone to Estradiol Androstenedione (4-dione) to testosterone
HSD17B2	Steroid metabolism	Estradiol to Estrone Testosterone to androstenedione (4-dione) 20alpha-hydroxyprogesterone to Progesterone
HSD17B3	Steroid metabolism	A-dione to Testosterone
HSD17B4	Lipid metabolism	Peroxisomal beta-oxidation for fatty acids
HSD17B5	Steroid metabolism	Aldo-keto reductase (AKR1C3) Conversion of aldehydes and ketones Reduction of prostaglandins Androstenedione (4-dione) to testosterone Bi-directional 3-alpha-, 17-beta- and 20-alpha HSD
HSD17B6	Steroid metabolism	3 alpha-adiol to dihydrotestosterone Androsterone to epi-androsterone
HSD17B7	Cholesterol synthesis Steroid metabolism	3-ketosteroid reductase Zymisterone to zymosterol Estrone to Estradiol
HSD17B8	Steroid metabolism	Estrone to Estradiol Testosterone to androstenedione (4-dione) Dihydrotestosterone to 3 alpha-adiol
HSD17B9	Retinol biosynthesis	Retinol Dehydrogenase 5 (RDH5) Final step in the biosynthesis of 11-cis retinaldehyde
HSD17B10	Oxidation of fatty acids and steroids Involved in tRNA maturation	3-hydroxyacyl-CoA dehydrogenase type II A subunit of mitochondrial ribonuclease P
HSD17B11	Metabolism of secondary alcohols and ketones	Short-chain alcohol dehydrogenase
HSD17B12	Lipid metabolism (fatty acid elongation) Steroid metabolism	3-ketoacul-coA reductase (KAR) Estrone to Estradiol
HSD17B13	Lipid metabolism	Oxidoreductase activity
HSD17B14	Lipid metabolism Steroid metabolism	Oxidoreductase activity Estradiol 17-beta-dehydrogenase activity

2.3.1 *Hydroxysteroid (17-beta) dehydrogenase type 12*

HSD17B12 is one member of this enzyme family. HSD17B12 was first characterized as KAR (Moon and Horton 2003). In addition, the HSD17B12 enzyme has been suggested to catalyze the conversion between E1 and E2 (Luu-The, Tremblay and Labrie 2006). Mouse HSD17B12 also catalyses the transformation of 4-androstenedione into testosterone (T) and of dehydroepiandrosterone (DHEA) into 5-androstene-3α, 17β-diol (3α-diol) (Blanchard and Luu-The 2007). The enzyme has been shown to be highly expressed in mature adipocytes

compared with preadipocytes in mouse (Bellemare et al. 2009) as well as in primate adipose tissue (Blanchard and Luu-The 2007). Adipose tissue is known to actively produce E2 locally, and therefore HSD17B12 has been speculated to be involved in the conversion of E1 to E2. In addition to its role in sex steroid metabolism, it is possible that the main function of HSD17B12 is in lipid metabolism, namely, in FA synthesis (Lukacik, Kavanagh and Oppermann 2006). Studies with zebrafish and *Caenorhabditis elegans* have also supported the role of HSD17B12 in the FA synthesis (Mindnich, Hrabe de Angelis and Adamski 2007, Entchev et al. 2008). Furthermore, *Hsd17b12* is at least partly regulated by sterol regulatory element-binding proteins, similar to many of the genes involved in lipid metabolism and FA and cholesterol biosynthesis (Nagasaki et al. 2009a).

In humans, HSD17B12 is expressed in various tissues and organs. The highest expression levels can be detected in heart, kidney, skeletal muscle, brain and liver. In addition, the enzyme is expressed in various steroidogenic tissues, such as the prostate, testis, adrenal gland, ovary and placenta (Sakurai et al. 2006). Recently, gene expression information has evolved, and *in silico* data (http://ist.medisapiens.com/#ENSG00000149084) have shown that the enzyme is extensively expressed throughout the human body. Luu-The and co-workers (2006) studied HSD17B12, HSD17B1 and HSD17B7 expression profiles in human estrogen-sensitive tissues, namely, mammary gland, ovary, uterus, vagina, cervix and placenta. Interestingly, HSD17B12 expression levels were high in all tissues except the placenta, were HSD17B1 was most highly expressed HSD17B enzyme. Due to the high expression levels of HSD17B12 in most estrogen-sensitive tissues, HSD17B12 was speculated to be the main enzyme participating in estrogen activation (Luu-The et al. 2006).

Interestingly, HSD17B12 possesses an activity similar to FAS, an enzyme complex responsible for *de novo* FA synthesis (Witkowski, Joshi and Smith 2002, Jayakumar, Chirala and Wakil 1997, Smith 1994). FAS has been extensively studied as a candidate target for cancer therapy (Lu and Archer 2005, Liu et al. 2002) and for the treatment of obesity (Loftus et al. 2000), suggesting that HSD17B12 may also be a candidate for those therapeutic targets. Thus, identifying the physiological and pathological roles of HSD17B12 may contribute to the development of treatments for cancers and metabolic disorders.

Song and others (Song et al. 2006) have found significant expression levels of HSD17B12 in breast cancer tissue samples. HSD17B12 was detected both in the cytoplasm and nuclei in these cells. In addition, there was found a significant correlation between HSD17B12 and ER-beta receptor expression in breast carcinoma samples. In addition, human cancer cell line studies (Smuc and Rizner 2009) showed that the expression levels of the HSD17B12 enzyme and ER re-

ceptors were positively correlated in breast and endometrial cancer cell lines, while the involvement of ERβ in the development and progression of breast carcinoma cells is currently unknown.

In contrast, recent studies have shown that the expression of HSD17B12 does not correlate with E2 levels in breast cancer tissue (Nagasaki et al. 2009b). Interestingly, HSD17B12 knockdown did not affect the E2 level in breast cancer cell lines, yet cell proliferation and growth was still affected (Day et al. 2008). Furthermore, Nagasaki and co-workers showed that the reduced breast cancer cell proliferation in the absence of HSD17B12 was rescued by the addition of AA, but not E2, to the cell culture. Thus, HSD17B12 affects cancer cell growth via EFAs, especially AA. Furthermore, most cancer cell lines express COX2, which is known to metabolize AA to PGs (Allaj, Guo and Nie 2013). Interestingly, in many cancer studies, high HSD17B12 expression levels are linked to a poor prognosis and lower survival rate of patients (Nagasaki et al. 2009b, Plourde et al. 2009).

While several studies have speculated about the function of HSD17B12 in breast cancer, only one article has addressed the function of HSD17B12 in ovarian cancer. This study showed that HSD17B12 was expressed in ovarian cancer (Szajnik et al. 2012). In that study, one hundred samples from untreated patients diagnosed with different epithelial ovarian cancer types (serous, mucinous and endometrioid) were studied. The authors concluded that strong staining for HSD17B12 correlated with a poor prognosis and poor outcome of patients with ovarian cancer. Thus, weak or moderate staining correlated with a better outcome. They also evaluated the function of HSD17B12 by silencing HSD17B12 expression by siRNA in an ovarian cancer cell culture. Interestingly, blocking HSD17B12 halted cell proliferation and induced apoptosis. In addition, the addition of AA to the cell culture rescued the phenotype, and the cells started to divide and apoptosis was stopped. In contrast, the addition of E2 had no effect on the phenotype.

2.4 Synthesis and elongation of fatty acids

The synthesis of FAs starts with the formation of malonyl-CoA. The cytosolic acetyl-CoA is carboxylated to malonyl-CoA, which then acts as a two-carbon donor throughout lipogenesis. In the cytosol, synthesis is catalysed by a multifunctional enzyme, FAS, which consumes the malonyl-CoA and NADPH to form palmitic acid in a cyclic synthesis of seven identical circles. During lipo-

genesis, palmitic acid (C16:0, saturated FA is formed and must be transformed in the ER for further elongation (Figure 11).

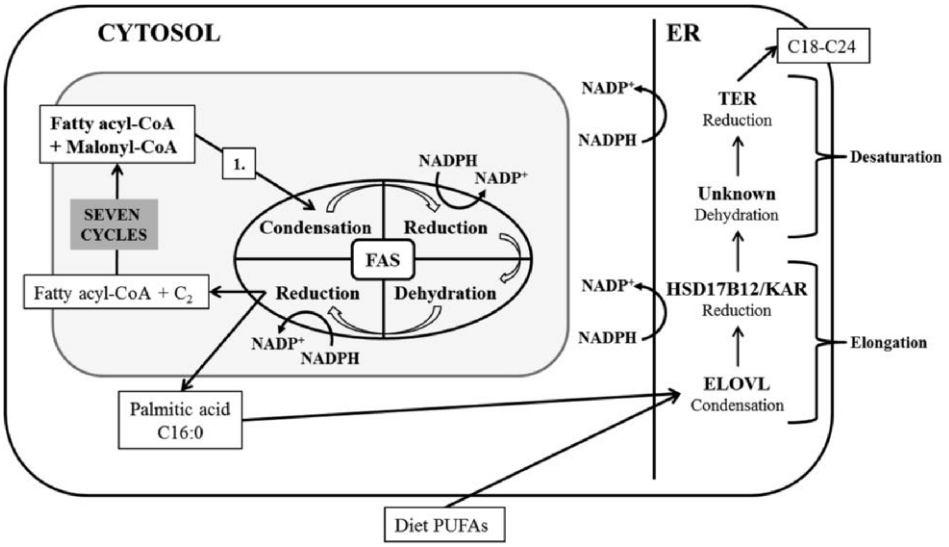

Figure 11. Synthesis and elongation of FA – synthesis of FAs occurs in the cytoplasm until palmitic acid (C16:0) is formed. In contrast, diet-based PUFAs and recently synthetized palmitic acids further elongate in the ER. *Modified from the thesis of Brolinson Annelie – Regulation of Elovl and fatty acid metabolism (2009)*

FA elongation of very long fatty acids (VLFAs) occurs in the ER. The synthesis is divided in two parts, elongation and desaturation. In addition, each part contains two enzymes: ELOVL (Ohno et al. 2010) and HSD17B12/KAR are expected to be responsible for elongation and a yet unknown dehydrase and TER (Moon and Horton 2003) are responsible for desaturation (Figure 11).

The rate-limiting step in VLFA elongation in normal conditions is the first step in elongation, which is catalysed by ELOVL enzymes. Seven ELOVL enzymes have been identified, and these enzymes differ by their tissue distribution and function (Wang et al. 2006). ELOVL1, 3 and 6 are responsible for the elongation of saturated and monounsaturated FAs, while ELOVL2, 4 and 5 are responsible for the elongation of polyunsaturated fatty acids (PUFAs). ELOVL5 also plays a role in elongating some monounsaturated FAs (Jump 2009). ELOVL1 and 3 are known to elongate very long (>C20) chain FAs. ELOVL2 catalyses the condensation of C20 and C22 PUFAs. ELOVL4 is responsible for elongating VLFAs

(>26). ELOVL5 has been shown to elongate a broad range of FAs; C16, C18 and C20 PUFAs and ELOVl6 elongate saturated FAs (C12-C16) (Moon, Hammer and Horton 2009).

2.4.1 *Elongation of diet-derived essential fatty acids*

EFAs are described as FAs that animal and human tissues are unable to synthetize and therefore must be obtained from the diet. EFAs comprise two main groups of PUFAs: omega-3 FAs (ω-3), in which the double bond is at the third carbon from the end of the chain; and omega-6 FAs (ω-6), in which the double bond is at the sixth carbon from the end of the chain (Simopoulos 2002). Linoleic acid (LA) is a precursor for ω-6 PUFAs and alpha-linolenic acid (ALA) for ω-3 PUFAs. LA and ALA are both obtained from the diet as triacylglycerols, which are hydrolysed in the gastrointestinal track lumen and, after hydroxylation, absorbed and packed in chylomicron phospholipids. Chylomicrons are then taken up by various tissues throughout the body. The liver is the most active tissue in the uptake of chylomicrons, especially in humans, and this function is crucial for less active tissues, such as the brain (Bézard et al. 1994). EFAs are stored in the outer layer of the cell membrane or used directly for PUFA synthesis in the ER. AA is the main storage form of PUFAs.

2.4.2 *Eicosanoids, the 20-carbon long fatty acids of PUFAs*

AA and its downstream metabolites are collectively described as eicosanoids. AA is metabolized by three main enzymes: COX, LOX and CYP450 (Figure 12). The COX pathway produces PGs: prostacyclins, TXs and hydroxy fatty acids. The LOX pathway is responsible for the formation of leukotrienes, lipoxins and hepoxins, and the CYP450 pathway forms epoxyeicosatraenoic acid and hydroxy fatty acids (Hyde and Missailidis 2009) (Figure 13).

Prostanoids are a subclass of eicosanoids containing PGs and thromboxanes (TXs) (Figure 13). PGs and TXs are metabolized from AA via the COX enzymes. COX-1 is known to be constitutively expressed in various tissues and is responsible for normal homeostasis; COX-2 is inducibly expressed, e.g., by a stimulus, such as inflammation and in cancer (Crofford 1997, Rouzer and Marnett 2009). A third COX enzyme, COX-3, has also been found. COX-3 is a splicing variant of COX-1 (Chandrasekharan et al. 2002).

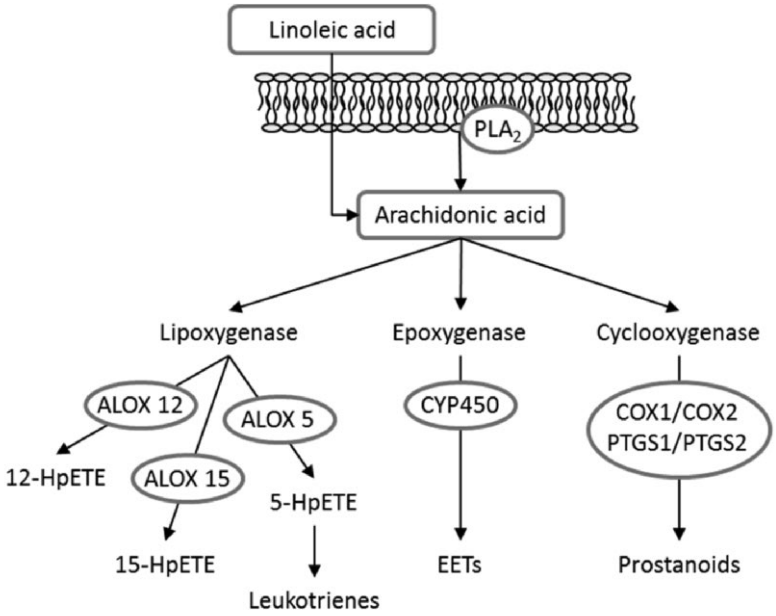

Figure 12. Schematic view of the eicosanoid pathway, and the three main pathways downstream of AA.

AA is stored at the cell membrane and esterified in phospholipids. When prostanoids are needed, these precursors are released from the cell membrane by the actions of one of three phospholipases (Funk 2001), namely, phospholipase A_2 (Pla_2), PLC and phospholipase D. Although there are three enzymes, Pla_2 is the only one that can release AA from the cell membrane directly in a single step reaction (Hyde and Missailidis 2009). AA is first metabolized with COX enzymes to PGH_2, which is then further metabolized to various different active forms of prostanoids. These active forms are then transported immediately out of the cell where they act locally, in the vicinity of the production cite. Prostanoids are very unstable, with some having a life-time of less than 30 seconds and those that are more stable being metabolized very quickly after secretion (Narumiya 2007).

2.4.2.1 Prostanoids and ovarian function

For ovarian function, the most important prostanoid is PGE_2, which acts via prostaglandin E receptors (EP). Each receptor has specific tissue distribution (Sugimoto and Narumiya 2007), and each receptor activates a specific secondary messenger pathway. Ovaries mostly express EP2 receptor ($EP2^{-/-}$ mice have been previously described in chapter 2.2.1). Another interesting finding is that EP3-, EP4-, thromboxane receptor (TP) and prostacyclin/ prostaglandin I receptor (IP)-deficient mice do not show any female infertility, despite the expression of these receptors in the reproductive track (Tilley et al. 1999).

2.5 Eicosanoids affect the nature of cancer

All eicosanoids are known to be bioactive lipids that are involved in normal development, inflammation and even cancer progression (Menter and Dubois 2012). AA and its downstream metabolites have been identified as active carcinogens or even tumour promoters (Hyde and Missailidis 2009).

Overexpression of COX enzymes has been linked to many different cancers. High expression levels have been documented in lung, breast, colorectal, prostate, head and neck, and ovarian cancer (Krysan et al. 2004, Barnes et al. 2006, Chan, Ogino and Fuchs 2007, Khor et al. 2007, Wang 2005, Uefuji, Ichikura and Mochizuki 2001, Hasegawa et al. 2005, Agarwal 2003, Qiu et al. 2014). In many cases, especially COX-2 overexpression has been linked to tumour metastatic activity. Recent studies have shown a link between tumour vascularization and elevated COX-2 expression (Hyde and Missailidis 2009). Increased PGE2 levels are especially positively correlated with increased levels of matrix metalloproteinase 9 (MMP-9), which, conversely, activates VEGF signalling.

Four different subtypes of LOX enzymes have been identified: 5-ALOX, 12-ALOX and 15-ALOX, which have two isoforms (15-ALOX-1 and 15-ALOX-2). Increased expression levels of LOX enzymes have been found in many different cancer types including breast, pancreatic, prostate, lung urinary bladder and colon (Moreno 2009, Schneider and Pozzi 2011). 5-ALOX and its AA downstream metabolite 5-HETE (Figure 13) in particular have been shown to activate VEGF signalling, leading to increased angiogenesis. ALOX is also related, especially in breast cancer, to the metastatic activity of cancer (Erez 2015).

The least studied AA pathway is the CYP450 pathway. Recent studies have shown that CYP450 produced EETs and HETEs can inhibit apoptosis via the

PI3/AKT signalling pathway, and 20-HETE has also been shown to induce VEGF-induced vascularization (Panigrahy et al. 2010, Hyde and Missailidis 2009).

2.5.1 *Eicosanoids and ovarian cancer*

Elevated expression of COX-2/PTGS2 has been reported in epithelial ovarian cancer and to be associated with a poor prognosis (Lee, Myung and Song 2013, Qiu et al. 2014). PGE_2 is one of the products that COX-2 metabolizes from AA. PGE_2 is typically very unstable and is inactivated very quickly after formation by 15-PGDH. Interestingly, the level of 15-PGDH is often decreased in cancer, leading to an accumulation of PGE_2, which has been shown to induce cell migration via upregulation of matrix metalloproteinase 2 (MMP2) and MMP9. In ovarian cancer, EGF has been shown to stimulate COX-2 and there by the product of PGE_2, and ovarian cancer cell migration (Qiu et al. 2014). Recent studies with human ovarian cancer cell lines (SKOV3 and OVCAR5) have shown that EGF-induced COX-2 expression is mediated via the PI3K/AKT signalling pathway (So et al. 2014).

In addition to COX-2, COX-1 may also play an important role in PGE_2 production in ovarian cancer cell lines (Kino et al. 2005). Kino and co-workers studied ten different epithelial ovarian cancer cell lines and found a positive correlation between COX-1 expression and the PGE_2 concentration, while COX-2 was undetectable. Interestingly, the use of a specific inhibitor of COX-1 in cell culture significantly decreased the concentration of PGE_2.

Although PGE_2 is known to promote epithelial cell migration in normal tissue, interestingly, it inhibits fibroblast migration (Sagana et al. 2009). The opposite effect of PGE_2 on cell migration depending on the cell type has been thought to be main reason the chemotherapy loses the efficacy. EP receptors can increase intracellular calcium (EP1) or cAMP (EP2 and EP4) or decrease intracellular cAMP levels (EP3) (Markovič et al. 2017). PTEN is a well-known tumour suppressor protein, and interestingly, it has been shown to regulate EP2 receptor activity in fibroblasts via positive feedback. In non-cancerous tissues, the activity of PTEN increases together with the levels of PGE_2. In this way, PTEN directly controls the number of functional EP2 receptors in fibroblasts. Sagana and co-workers (2009) showed that PTEN directly regulates EP2 receptor expression via cAMP and thus regulates fibroblast activity. In cancer, the expression of PTEN is often downregulated, leading to increased activity of EP2 receptors and consequently to increased cell migration ability (Sagana et al. 2009).

Although ovarian cancer is extensively studied, the mechanism by which the cancer becomes resistant to treatments is still unknown. In ovarian and breast cancer, the main reason that chemotherapy does not work is that the cancer cells become resistant to drug-induced apoptosis. COX-2 overexpression is known to reduce apoptosis, increase cell proliferation and stimulate angiogenesis (Ali-Fehmi et al. 2005). Interestingly, COX-2 has also been suggested to regulate the expression of survivin in cancer cells (Athanassiadou et al. 2008). Survivin is an anti-apoptotic protein that is normally observed in embryonic and fetal development, but it is not detected in adults. In addition, survivin has been shown to affect FSH-stimulated VEGF expression in ovarian cancer, and interestingly, survivin has been thought to antagonize FSH and lead to increased VEGF expression (Huang et al. 2008). Huang and co-workers showed a clear correlation between increased VEGF levels and activated PI3K/AKT signalling. In serous adenocarcinoma, they detected a positive correlation between FSH-induced survivin and phosphorylated AKT. Furthermore, the survivin and AKT levels were correlated with the 5-year survival of patients. Based on these findings, the survivin and PI3K/AKT pathways are thought to be at least one important mechanism underlying the development of drug-resistance (Xing et al. 2008).

3 AIMS OF THE STUDY

The main aim of this thesis was to identify the physiological role of the HSD17B12 enzyme. The tissue distribution of the HSD17B12 enzyme in mouse is known to mimic the human tissue distribution. Therefore, to study the function of the enzyme, a knockout mouse model was generated and characterized. **In addition, the expression of HSD17B12 in human ovaries and ovarian cancer was studied.** Identifying the physiological and pathophysiological function of the HSD17B12 enzyme is especially interesting because HSD17B12 might function as a drug target candidate for the treatment of cancers, especially ovarian cancer.

The specific aims of the thesis are as follows:

1. *To study the role of the HSD17B12 enzyme in embryonic development*

2. *To study the role of* the *HSD17B12 enzyme in ovarian function and in female fertility*

3. *To study the role of* the *HSD17B12 enzyme in ovarian cancer*

4 MATERIALS AND METHODS

4.1 Experimental animals

4.1.1 *Generation of HSD17B12$^{+/-}$ and HSD17B12$^{-/-}$ mice (I, II)*

Table 2 Commercial gene traps used to generate the HSD17B12 knockout mice (HSD17B12$^{-/-}$) and mice with one functional HSD17B12 allele (HSD17B12$^{+/-}$) **(I, II)**

Gene trap clone	*Manufacture*	*Location*	*Used in*
AO3OEO6	German Gene Trap Consortium (Munich, Germany)	Intron 3	I, II
DC0186	Sanger Institute (Hinxton, UK)	Intron 1	II

The gene trap clone AO3OEO6 (mouse line B) was obtained from the German Gene Trap Consortium (Munich, Germany), and the gene trap clone DC0186 (mouse line A) was from Sanger Institute (Hinxton, UK).

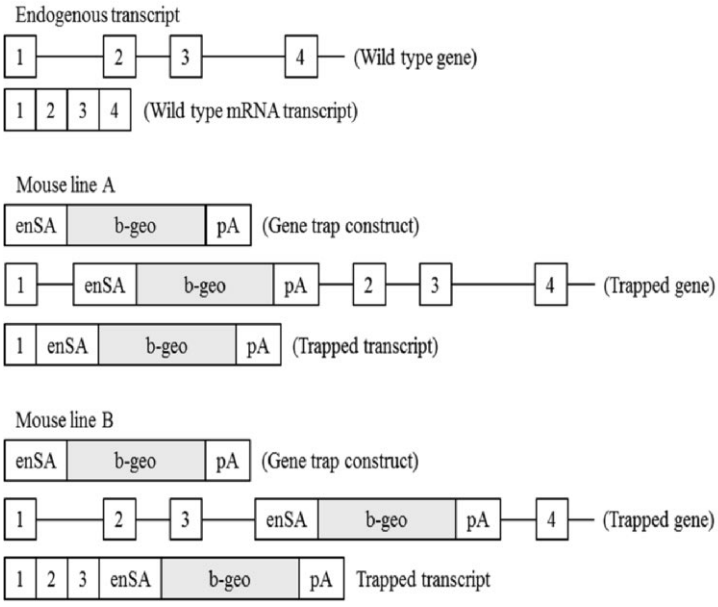

Figure 13. Schematic view of two different commercial gene traps used to generate HSD17B12-deficient mouse lines. Mouse line A – trap DC0186, from Sanger and mouse line B – trap AO3OEO6, from GGTC.

The ES cells were injected into C57BL/N6 mouse blastocysts to generate chimeric mice. Breeding of the chimeras with C57BL/N6 mice produced HSD17B12$^{+/-}$ mice with one functional HSD17B12 allele and one trapped allele. The mice used had a mixed (129/C57BL/6N, 1:1) genetic background and wild type (WT) littermates were used as controls in all studies.

The mice were housed in specific pathogen-free conditions at Central Animal Laboratory, University of Turku, in compliance with international guidelines on the care and use of laboratory animals. The mice were given soy-free natural ingredient feed (Special Diets Services, Witham, UK). All animal studies were conducted in accordance with the Finnish Animal Ethics Committee and the Institutional animal care policies of the University of Turku (Turku, Finland), complying with international guidelines on the care and use of laboratory animals.

4.1.2 *Genotyping of HSD17B12$^{+/-}$ and HSD17B12$^{-/-}$ mice (I, II)*

Genotyping of the mice was carried out with DNA extracted from the yolk sacs at E7.5-E9.5 or ear marks of 2-wk-old mice.

The primer pair WT forward/ WT reverse amplified an 1100-bp fragment in both heterozygous and wild-type (WT) mice, whereas the primer pair WT forward/ KO reverse amplified a 420-bp fragment in heterozygous and HSD17B12$^{-/-}$ mice. The HSD17B12$^{+/-}$ mice was also identified by primers that amplified a 480-bp internal fragment of the *lacZ* reporter gene.

Table 3 Genotyping primers and PCR conditions

HSD17B12$^{-/-}$	**Sequence**	**Product (bp)**	**Ta (°C)**	**Study**
WT forward	AATCGACAAATGGGACCTAATG	1100	60	I
WT reverse	AGCCAATTACAGAGAGCAGAGG			
KO reverse	CGTGTCCTACAACACACAATACAACC	420	60	I

HSD17B12$^{+/-}$	**Sequence**	**Product (bp)**	**Ta (°C)**	**Study**
Reporter – forward	TACGATGCGCCCATCTACAC	480	60	II
Reporter – reverse	TACCCGTAGGTAGTCACGCA			

4.1.3 *Breeding test and estrous cycle determination (II)*

The fertility of HSD17B12$^{+/-}$ mice was analysed by breeding 10 HSD17B12$^{+/-}$ females with WT males, 10 WT females with HSD17B12$^{+/-}$ males and four WT females with WT males. The litter sizes and the frequency of litters born were followed for 5 months. Vaginal smears were collected in PBS from 10 HSD17B12$^{+/-}$ and 10 WT females for a period of 50 days to determine the estrous cycle. The smears were air-dried on microscopic slides, fixed with ethanol and stained with Mayer's hematoxylin. The phase of the estrous cycle was then detected by cytology.

4.2 Histological analyses

4.2.1 *Embryos and ovarian histology (mouse) (I, II)*

E6.5-E8.5 embryos were isolated in ice-cold PBS and fixed overnight in 4% paraformaldehyde (PFA) at +4C. Ovaries from 3-month-old mice (8 HSD17B12$^{+/-}$ and 9 WT) were collected at diestrous and fixed in 10% formalin at RT overnight. Both embryos and ovaries were dehydrated and embedded in paraffin using the same protocol. Thereafter, serial 4µm-thick sections were cut, deparaffinized, rehydrated and stained with hematoxylin and eosin (HE).

For quantitation, all ovarian samples were cut (WT, 220 ± 16 sections per ovary; HSD17B12$^{+/-}$, 217 ± 15 sections per ovary). All sections were analysed to assess the histological changes in HSD17B12$^{+/-}$ ovaries (polyovular follicles - POFs, trapped oocytes – TOs and meiotic spindles).

4.2.2 *Human ovarian histology (II, III)*

Human ovarian tissue samples were collected from consenting women undergoing elective caesarean sections at the Karolinska University Hospital Huddinge (Sweden). The thin cortical tissue samples were freshly fixed in 4% PFA at +4°C overnight, dehydrated, embedded in paraffin, and processed into serial 4-µm-thick tissue sections. The study protocol was approved by the Stockholm region ethics board. Stained slides were digitized with a Panoramic 250 Flash scanning microscope (3Dhistech, Budapest, Hungary) and viewed and analysed with Panoramic Viewer software (3Dhistech, Budapest, Hungary).

The in-house collection of tumour specimens was approved by the Turku University Hospital ethics committee. The ovarian tumour tissue microarray (TMA) consisted of 108 different cystadenocarcinoma tumours of various histology (42 serous, 31 mucinous and 35 endometrioid) and 50 different ovarian adenomas (including mucinous, serous and borderline serous adenoma). Four micron-thick sections of formalin-fixed, paraffin-embedded tissue specimens were used for immunohistochemical staining.

In addition, formalin-fixed commercial TMAs (5µm-thick-sections) and paraffin-embedded ovarian carcinomas were used (TMA - OV1005a, US Biomax, Inc., Rockville, MD, USA). The TMA included information regarding the FIGO stage, TNM and pathological grade of the specimens which included ovary serous adenocarcinoma (n=27), ovary mucinous adenocarcinoma (n=3), ovary endometrioid adenocarcinoma (n=10), ovary transitional cell carcinoma (n=5), ovary metastatic carcinoma (n=10), ovary adenoma (n=25, including mucinous, serous and borderline serous adenoma), adjacent normal ovary tissue (n=17) and normal ovary tissue (n=3) samples. The detailed information for all samples used in this study and the ages of the patients are shown in Table 3.

Table 4 Description of human ovarian samples (III)

Age (median and range)	**53 years (16 - 89 years)**			
		Number of samples		
Malignant/ Borderline specimens Histological subtype	**Age (median and range)**	**ELOVL5**	**HSD17B12**	**COX2**
Serous adenocarcinoma	56 years (22 -82 years)	77	69	72
Mucinous adenocarcinoma	57 years (34 - 82 years)	37	32	43
Endometrioid adenocarcinoma	55 years (27 - 77 years	48	45	45
Transitional cell carcinoma	49 years (38 - 66 years)	5	5	5
Metastatic carcinoma	52 years (28 - 65 years)	10	10	10
Borderline serous cystadenoma	55 years (22 - 84 years)	31	20	29
All samples	**55 years (22 - 84 years)**	**208**	**181**	**204**

Benign	**48 years (16 - 89 years)**	**ELOVL5**	**HSD17B12**	**COX2**
Normal ovarian tissue adjacent to cancer tissue	48 years (29 - 63 years)	17	17	17
Serous cystadenoma	55 years (16 - 89 years)	33	26	22
Mucinous cystadenoma	44 years (17 - 83 years)	27	28	26
All samples	**48 years (16 - 89 years)**	**77**	**71**	**65**

4.2.3 *Beta-galactosidase staining (I)*

To visualize the expression of the fusion gene, E7.5-E9.5 embryos were studied. The embryos were dissected, washed in PBS, and fixed for 60 min in fixative containing 0.2% glutaraldehyde, 2 mM MgCl2, and 5 mM EGTA in PBS (pH 7.3). Embryos were washed in washing buffer containing 0.02% Nonidet P-40, 2 mM MgCl2, and 0.01% nadeoxycholate in PBS (pH 7.3) three times for 3 min and incubated overnight at +4 C (or 3 hours at +37°C) with β-galactosidase substrate (X-gal; 1 mg/ml; Fermentas, Hanover, MD) in washing buffer supplemented with 5 mM potassium ferrocyanide and 5 mM potassium ferricyanide. The stained embryos were further fixed for 2 hours in 4% PFA at room temperature, washed with PBS, and photographed.

4.2.4 *Whole-mount mammary gland staining (II)*

Mammary glands were collected from 3-month-old mice and spread out on microscope slides to mimic the normal shape of the tissue in the mouse. The glands were fixed with a 3:1 mixture of 100% ethanol and acetic acid at +4°C overnight. The next day, the glands were washed with 70% ethanol for 30 minutes, rinsed in water and stained with Carmine Alum (1 g carmine and 2.5 g aluminum potassium sulfate, Sigma, St Louis, MO in 500 ml water) at +4°C overnight. The tissues were dehydrated with increasing concentrations of alcohol and finally with xylene for three days. The slides were mounted with PERTEX® (Histolab Products AB, Gothenburg, Sweden). For quantification, the glands were imaged with a stereomicroscope, and the branches of the mammary gland duct were counted using the ImageJ program.

4.2.5 *Immunohistochemistry and immunofluorescence (II, III)*

Human and mouse ovarian sections as well as TMA sections were deparaffinized and rehydrated using a series of 5-minute washes in xylene (x3), 100% ethanol (x2), 96% ethanol (x2), 70% ethanol (x2) and dH2O (x3). Heat-induced epitope retrieval (HIER) was performed on a pressure cooker (2100-RETRIVER, PickCell Laboratories, Amsterdam, Netherlands) for 2.5 hours in citrate buffer (pH 6.0), and the slides were washed twice for 5 minutes in PBST (1x PBS + 0.05% Tween). The sections were then circumscribed with an *ImmEdge*™ Pen (H-4000, Vector Laboratories, Burlingame, CA) and incubated for 10 minutes with 3% BSA + 10% NGS (normal goat serum) in PBST at RT in a humid

chamber. The sections were then incubated overnight with one of the primary antibodies (Table 4) in 3% BSA + 10% NGS in PBST at 4°C.

In addition, human and mouse ovarian sections were incubated with a mixture of purified HSD17B12 protein fragment (Table 4) and an excess of antigen was used to test the nonspecific binding of the primary antibody.

On the following day, endogenous peroxidase activity was blocked with 3% H2O2 (Sigma-Aldrich, St. Louis, MO) treatment (20 minutes, RT). After washing, the sections were incubated for 1 hour with secondary antibody (Table 5) at RT. To detect peroxidase, 3,3'-diaminobenzidine (DAB) was used (Liquid DAB + Substrate Chromogen System, DAKO, Copenhagen, Denmark), and the sections were counterstained with MAYERS HTX Histolab (Histolab Products AB, Gothenburg, Sweden). Finally, the sections were dehydrated using a series of washes in 96% ethanol (2 x 3min), 100% ethanol (2 x 3 minutes) and xylene (3 x 5 minutes) and mounted with PERTEX® (Histolab Products AB, Gothenburg, Sweden).

For immunofluorescence, mouse ovarian sections were incubated overnight with primary antibody against α-tubulin (Table 4) in 3% BSA + 10% NGS in PBST at 4°C. On the following day, the sections were washed with PBST and incubated for 1 hour with secondary antibody (Table 5) in PBST at RT. The slides were washed with PBST and finally mounted with VECTASHIELD® Hard Set Mounting Medium with DAPI (Vector Laboratories, Burlingame, CA).

Table 5 Primary antibodies used in studies I, II, III

Target	***Manufacturer, catalog #***	***Dilution used***	***Application***	***Used in***
HSD17B12	Atlas Antibodies, Stockholm, Sweden, # HPA016427	For human: 1,7 ug/ml (1:60) For mouse 0,8 ug/ml (1:120)	IHC, WB	II, III
ELOVL5	ThermoFisher Scientific, Waltham, MA, USA, #PA5-32741	6,7 ug/ml (1:150)	IHC	III
COX2	ThermoFisher Scientific, Waltham, MA, USA, #PA5-16817	0,3 µg/ml (1:600)	IHC	III
Tubulin alpha	LabVision-NeoMarker, Tubulin-alpha Ab-2, Clone DM1A	0.2ug/ml (1:1000)	IF	II
GAPDH	HyTest Ltd, anti-GAPDH, Cat. 5G4 Mab 6C5	0.3 µg/ml (1:1000)	WB	II
PrEST Antigen HSD17B12	Atlas Antibodies, Stockholm, Sweden (APrEST73031)	1:2 of #HPA016427	IHC	II

Table 6 Secondary antibodies used in study II

Antibody	*Manufacture*	*Dilution used*	*Application*	*Used in*
Alexa fluor 488 (Goat-antimouse IgG)	Life Technologies	1:500	IF	II
Antirabbit IgG, HPR-linked secondary antibody	Cell Signaling Technology, Danvers, MA	1:3000	WB	II

4.3 Western blot analysis (II)

For native Western blotting, tissues (mouse WT ovary and HSD17B12$^{+/-}$ ovary) were homogenized in cold homogenization buffer (RIPA –150 mM Tris-HCl, pH7.4; 1% NP-40, 150 mM NaCl, 0,5% NaDeoxycholate, 1 mM EDTA and 1 mM SDS) with ULTRA-TURRAX® on ice. Homogenates were incubated on ice for 30 minutes and mixed occasionally. The lysates were centrifuged at 12 000 g for 20 minutes at +4°C. Supernatants were removed, and the protein concentration was determined with a BCA kit (Pierce™ BCA Protein Assay Kit, Thermo Scientific, Waltham, MA) according to the manufacturer's instructions. Samples were diluted to equal protein concentrations and combined with 4x SDS sample buffer without β-mercaptoethanol (125 mM Tris-HCL, pH 6.8, 300 mM SDS, 40% glycerol, 0.6 mM bromophenol blue). Protein samples (30 µg/well) and molecular weight marker (Precision Plus Protein™ Standard, Dual Color, BIO-RAD, Berkley, CA) were separated by using commercial precast gels (Mini-Protein® TGX™ Gels, BIO-RAD, Berkley, CA) first for 10 minutes at 50 V, followed by 60 minutes at 100 V. Proteins were transferred to PVDF blotting membrane (Amersham™ Hybond™ P 0.45 PVDF, GE Healthcare, Life Science, Buckinghamshire, UK) using the BIO-RAD TRANS-BLOT® TURBO™ transfer system for 30 minutes at 25 V. All the following steps were performed with gentle agitation. Membranes were blocked with 5% non-fat milk (Fat-Free Milk powder, Valio, Finland) in PBST (PBS + 0.1% Tween) for 60 minutes at RT. Membranes were then incubated with primary antibody (Table 4) or with housekeeping protein antibody (Table 4) in 5% non-fat milk in PBST at +4°C overnight. Membranes were warmed to RT and incubated for 60 minutes, and then washed three times for 10 minutes with PBST at RT. The secondary antibody (Table 5) in PBST was incubated with the membranes for 60 minutes at RT. Finally, the membranes were exposed to Western Lightning® ECL Pro reagent (PerkinElmer, Inc., Waltham, MA) for 1 minute at RT and visualized using a LAS-4000 (FUJIFILM).

4.4 *In vitro* blastocyst culture (I)

Heterozygous mice with one disrupted allele (HSD17B12$^{+/-}$) were mated, and E3.5 embryos were collected by flushing the uteri of pregnant females. Blastocysts were cultured individually in ES cell medium without leukemia inhibitory factor on gelatin or feeder cells (Life Technologies, Inc., Invitrogen, Carlsbad, CA) in 5% CO2 at 37°C. The expansion and growth of the ICM was followed for 7 day, after which the cultured cells were genotyped.

4.5 Gene expression analyses

4.5.1 *RNA isolation and quantitative real-time RT-PCR (I, II)*

For quantitative real-time RT-PCR (qRT-PCR) analyses, mouse ovaries were collected at the diestrous phase of the estrus cycle. Total RNA extracted using TRIsure reagent according to the manufacturer's instructions (Bioline reagents, London, UK), and the RNA was treated with deoxyribonuclease (DNase) I (DNase I Amplification Grade Kit; Invitrogen Life Technologies, Paisley, UK). Reverse transcription PCR was carried out using the DyNAmo cDNA synthesis kit (Thermo Scientific, Waltham, MA), and quantitative PCR was performed using the DyNAmo Flash SYBR Green qPCR kit (Thermo Scientific, Waltham, MA).

Table 7 RT-qPCR primers and PCR condition used in studies I, II

Gene	Sequence	Product (bp)	Ta (°C)	Study
Hsd17b12	ACCAAAACGTGGAATGAAGATT TTTCTTGATGGTGTTGTCCAAG	250	60	I, II
L19	CTGAAGGTCAAAGGGAATGTG GGACAGAGTCTTGATGATCTC	250	60	I, II

4.5.2 *Whole-genome microarray (II)*

Microarray analyses were made for WT (n = 6) and HSD17B12$^{+/-}$ (n = 6) mice at the diestrous at age of 2 months. The microarray experiments were carried out at the Finnish DNA Microarray and Sequencing Centre, Turku Centre for Biotech-

nology using the MouseWG-6 v2 Expression BeadChip (Illumina, San Diego, CA) which contains a total of 48 000 probes (Shi et al. 2006).

Normalization of the microarray data was performed using quantile normalization. Differentially expressed genes were identified using the Limma-package in the statistical software R (http://r-project.org). The level of statistical significance was set at $P < .05$ to identify up- and down-regulated genes. Pathway analyses were carried out at the Finnish DNA Microarray and Sequencing Centre using the KEGG (Kyoto Encyclopedia of Genes and Genomes) database, for which a false discovery rate (FDR) was used as the cut-off for pathway enrichment. Data from single cell human oocyte DNA sequencing were acquired from the European Nucleotide Archive (accession code PRJEB8994) and aligned to the human genome (version hg18) using tophat2/ bowtie2 (Kim et al. 2013, Langmead and Salzberg 2012). Tags were annotated and counted within the gene bodies using Homer and then imported into R (Heinz et al. 2010). Tag counts were transformed to log2 counts per million reads and plotted with ggplot2.

4.6 Measurements of biologically active products

4.6.1 *Measurement of reproductive hormones (II)*

We measured the uterus wet weight and ovarian weight and collected blood samples from WT (n = 10) and HSD17B12$^{+/-}$ (n = 10) female mice at 3 months of age at diestrous. The serum was stored at –20°C until used. Serum follicle-stimulating hormone (FSH) and luteinizing hormone (LH) concentrations were measured by immunofluorometric assays as described previously (Haavisto et al. 1993, van Casteren, Schoonen and Kloosterboer 2000) and prolactin (PRL) was assessed using the DuoSet® ELISA Developmental kit (R&D Systems, Inc.) for mouse PRL (Krol et al. 2011). E2, E1, A-dione, T and progesterone (P4) were analysed in serum and ovarian samples using a gas chromatography tandem mass spectrometry method (Nilsson et al. 2015). For intra tissue measurements of E2, E1 and P4 the ovaries (10 HSD17B12$^{+/-}$ and 8 WT) were collected at diestrous and homogenized in sterile water (1 whole ovary/0.5 ml), and the homogenates were used for analysis.

4.6.2 *Fatty acid measurements from ES cells (I)*

Blastocysts (E3.5) were used to isolate ES cells, and blastocysts were cultured *in vitro* (Bryja et al. 2006*)*. Lipids were extracted using the modified Folch method (FOLCH, LEES and SLOANE STANLEY 1957), in which FA formed the methyl esters and the esters were prepared from the lipid extracts at 92°C by boron trifluoride-catalysed transesterification (MORRISON and SMITH 1964, Agren, Julkunen and Penttilä 1992) The esters were dissolved and analysed by gas chromatography with flame ionization detection (AutoSystem; PerkinElmer, Norwalk, CT). The LA and AA were identified with help of FA methyl ester mixtures 68D and 37 obtained from -Check Prep, Inc. (Elysian, MN), and Supelco (Bellefonte, PA), respectively.

4.6.3 *Measurement of eicosanoids and oxidized fatty acids (prostaglandins) (II)*

Ovarian samples from 3-month-old mice (10 HSD17B12$^{+/-}$ and 10 WT) were collected at diestrous, snap frozen in liquid nitrogen and stored at –80°C for further analyses. Eicosanoids and other oxidized PUFAs were extracted from samples with aqueous acetonitrile that contained deuterated internal standards. The metabolites AA, 6-keto prostaglandin F1alpha (6 ketoPGF1α), prostaglandin D2 (PGD2), PGE2, PGF2α, and thromboxane B2 (TXB2) were determined by HPLC-tandem mass spectrometry (LC-MS/MS) with Multiple Reaction Monitoring (MRM) in negative mode using a ABSciex 4000 QTrap® mass spectrometer with electrospray ionization (Applied Biosystems/ MDS Analytical Technologies, Darmstadt, Germany). The LCMS/ MS method used for the analytical determination of eicosanoids has been published (Unterwurzacher et al. 2008).

4.7 Statistics (I, II, III)

Hotelling's T2 -test was used to evaluate differences in multivariate means of AA, 6 keto PGF1a, PGD2, PGE2, PGF2a, and TXB2 concentrations in the ovary between WT and HSD17B12$^{+/-}$ mice. Testing was conducted using R statistical software (R Development Core Team. R: A language and environment for statistical computing. Rstatistical software version 3.0.1; 2013. Available from: http://www.R-project.org) with the package 'Hotelling' (Curran, JM. Hotelling: Hotelling's T-squared test and variants; R package version 1.0 –2; 2013. Available from: http://cran.r-project.org/web/packages/Hotelling/). The significance of

the presence and absence of PO (polyovular follicle), M (meiotic spindle) and TO (trapped oocyte) in WT and HSD17B12$^{+/-}$ mice was tested using Fisher's Exact test. Due to the frequent absence of occurrences in WT mice, the data were binarized into observed/nonobserved occurrence of an event.

Other statistical analyses were carried out with Microsoft Excel or SigmaPlot/Stat (Systat Software, Erkrath, Germany). Statistical significance between groups was determined with Student's *t* test, the Mann-Whitney test or ANOVA. Significance was determined as $P < .05$, and the results are presented as the means ± standard error of the mean (SEM).

4.7.1 *Quantitation of immunohistochemistry and statistical analyses (III)*

The stained slides were digitized with a Panoramic 250 Flash scanning microscope (3DHISTECH), intensities were quantified with QuantCenter from 3DHISTECH Ltd (Budapest, Hungary), and the results were confirmed manually. Statistical analyses were carried out with GraphPad Prism (GraphPad Software, CA, USA). Depending on the analysis, statistical significance between groups was determined with Student's *t* test, the Mann-Whitney test, linear regression or ANOVA. The significance level was determined as $P < 0.05$, and the results are presented as the means ± standard error of mean (SEM).

5 RESULTS

5.1 Generation of the HSD17B12$^{-/-}$ mouse line (I, II)

To study the function of the HSD17B12 enzyme, a knock-out mouse line was generated. Two mouse lines were initially generated to disrupt the mouse *Hsd17b12* gene with commercially available embryonal stem (ES) cell lines. The gene trap in ES cells from Sanger Institute (DC0186) was localized in intron one (between exons one and two), and the gene trap in ES cells from the German Gene Trap Consortium (AO3OEO6) was localized in intron three (between exons three and four). In both mouse lines, the fusion protein contained b-geo, allowing the study of the gene expression of HSD17B12 by beta-galactosidase staining. In addition, both of these two mouse line showed identical results, while most of the studies were carried out using the ES cells obtained from the Sanger Institute.

5.2 Fully functional HSD17B12 is essential for normal ovarian function and embryonic development (I, II)

5.2.1 *The HSD17B12 gene is widely expressed in both mouse and human ovaries (II)*

Immunohistochemical analyses localized HSD17B12 in both mouse and human ovaries in the oocyte, granulosa cells, theca interna, corpus luteum and surface epithelium. In both species, the most intensive staining was observed in the *corpus luteum*. In human ovaries, the theca interna was also intensively stained. In addition, the ovaries of HSD171B12$^{+/-}$ mice showed weaker HSD17B12 expression than WT ovaries. The lower HSD17B12 expression in these mice was further confirmed by Western blot analyses. The WT mouse ovaries showed strong staining of a 68-kD protein, whereas HSD17B12$^{+/-}$ mouse ovaries showed about half the staining intensity of the protein. The HSD17B12 expression levels were also studied by qRT-PCR, and again HSD17B12$^{+/-}$ ovaries showed half of the HSD17B12 expression level of that observed in WT ovaries. HSD17B12 expression analysed by qRT-PCR was also altered according to the estrous cycle phase, and the highest levels were detected in diestrous and in pseudopregnant ovaries.

5.2.2 *HSD17B12$^{+/-}$ females showed decreased fertility and prolonged estrous cycle (II)*

Interestingly, the HSD17B12 +/- males were fully fertile, while the females had multiple fertility problems. The HSD17B12+/- females gave birth at a random frequency, while the WT female litters were born regularly between 22 days. In addition, the HSD17B12+/- females also had smaller litters compared with WT females when both of them were mated with WT male mice. Vaginal smear analyses showed a significantly prolonged estrous cycle in HSD17B12+/- females, consistent with the increased time between litters. Females had an especially increased diestrous phase, which varied from 2 to 45 days. Because the ductal branching of the mammary gland is known to be regulated at puberty by the cyclic changes in E2 and P4, the mammary glands of HSD17B12+/- mice were studied at the age of 3 months. In accordance with the prolonged estrous cycle, the HSD17B12+/- females showed significantly fewer numbers of ductal branches than WT female mammary glands.

5.2.3 *HSD17B12$^{+/-}$ females showed dysfunction in oogenesis and ovulation (II)*

Both HSD17B12$^{+/-}$ and WT ovaries contained all the different stages of follicles, and CLs were also present. In addition, there were no differences in the weight and size of the ovaries between the genotypes. Nevertheless, HSD17B12$^{+/-}$ ovaries had multiple defects. HSD17B12$^{+/-}$ females had an increased number of polyovular follicles in ovaries (figure 14A), varying from one to three polyovular follicles in each ovary, while one polyovular follicle was found in one of the nine WT ovaries. Polyovular follicles are often formed as a consequence of dysfunction in germinal cyst breakdown, and thus the ovaries at the postnatal day (PND) three were analysed for the formation of primordial follicles. Interestingly, there were no differences between the genotypes.

In addition, HSD17B12$^{+/-}$ ovaries showed trapped oocytes (TO, figure 14B), i.e., the oocyte remained inside the luteinizing granulosa/theca cells after ovulation, further indicating the dysfunction in follicular wall breakdown during ovulation. Seven of eight HSD17B12$^{+/-}$ ovaries had one to three TOs, whereas the WT ovaries had none.

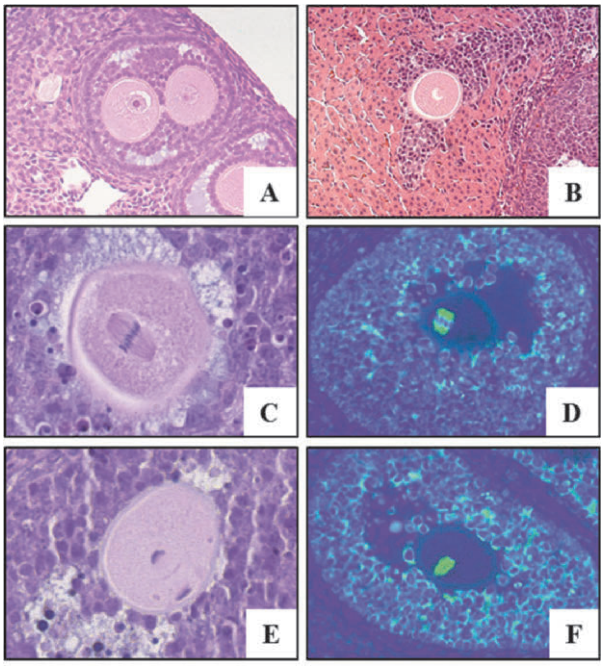

Figure 14. Histological defects observed in HSD17B12$^{+/-}$ ovaries **A**, Polyovular follicle seen in HSD17B12$^{+/-}$ ovaries. **B**, Oocyte trapped inside the luteinizing granulosa cells. **C** and **D**, Meiotic spindle (metaphase) with pyknotic cells observed around the oocyte, indicating apoptosis. **E** and **F**, Meiotic spindle (anaphase). *Modified from Kemiläinen at al. 2016*

Interestingly, the HSD17B12$^{+/-}$ female ovaries showed a disrupted regulation of the meiotic arrest of oocytes (figure 14C-F). In HSD17B12$^{+/-}$ ovaries, meiotic spindles at metaphase and even a few spindles at anaphase could be detected at the diestrous phase, and interestingly, already in secondary follicles. To further study the defect in meiotic arrest, the size of the follicles with meiotic spindles was measured and compared with the fully mature antral follicles from WT ovaries. According to the measurements, the follicles containing the meiotic spindles were not mature, and spindles were found only in the atretic follicle, indicating that the premature resumption of meiosis leads to follicular atrophy. The presence of meiotic spindles was confirmed by HE and double immunofluorescence (α-tubulin and 4',6-diamino-2-phenylindole) staining.

A whole-genome microarray study of the mouse transcriptome further supported our results showing the disturbance of meiotic arrest. The pathway analyses showed that in HSD17B12$^{+/-}$ ovaries, genes related to the control of meiosis were significantly affected. Additionally and interestingly, several genes related to meiotic arrest were downregulated, whereas the meiotic activators were upregulated. Table 4 shows several other interesting genes that were significantly differently expressed in HSD17B12$^{+/-}$ ovaries compared with WT according to our microarray study.

Table 8. Microarray results: A list of several interesting genes that are significantly differently ($p < 0.05$) expressed in HSD17B12$^{+/-}$ and WT ovaries .

Symbol	FC	Definition
Pla2	1,841	Mus musculus phospholipase A2, group IVF (Pla2g4f), mRNA.
Fads2	1,82	Mus musculus fatty acid desaturase 2 (Fads2), mRNA.
Fads3	1,475	Mus musculus fatty acid desaturase 3 (Fads3), mRNA.
Elovl1	1,482	Mus musculus elongation of very long chain fatty acids 1 (Elovl1), mRNA.
Elovl6	-1,469	Mus musculus ELOVL family member 6 (Elovl6), mRNA.
Alox5	1,372	Mus musculus arachidonate 5-lipoxygenase (Alox5), mRNA
Ptgs1	1,174	Mus musculus prostaglandin-endoperoxide synthase 1 (Ptgs1), mRNA.
Ptges	1,842	Mus musculus prostaglandin E synthase (Ptges), mRNA.
Aurka	1,571	Mus musculus aurora kinase A (Aurka), mRNA.
Mos	1,625	Mus musculus Moloney sarcoma oncogene (Mos), mRNA.
Skp1a	-1,895	Mus musculus S-phase kinase-associated protein 1A (Skp1a), mRNA.
Cdc20	1,864	Mus musculus cell division cycle 20 homolog (S. cerevisiae) (Cdc20), mRNA.
Kiss1	2	Mus musculus KiSS-1 metastasis-suppressor, mRNA
Erbeta	-2,6	Mus musculus estrogen receptor 2 (beta) (Esr2)
GJA1	-1,4	Mus musculus gap junction membrane channel protein alpha 1 (Gja1)
GJA4	1,8	Mus musculus gap junction protein, alpha 4 (Gja4)
Pten	-1,5	Mus musculus phosphatase and tensin homolog (Pten)
Rb1	-1,9	Mus musculus retinoblastoma 1 (Rb1)
Ckmt1	1,9	Mus musculus creatine kinase, mitochondrial 1, ubiquitous (Ckmt1), nuclear gene encoding mitochondrial protein
Sdc1	2,1	Mus musculus syndecan 1 (Sdc1)
Cldn3	2	Mus musculus claudin 3 (Cldn3)
Gpr172b	1,8	Mus musculus G protein-coupled receptor 172B (Gpr172b)

5.2.4 *HSD17B12 in early embryonal development of mice (I)*

HSD17B12$^{+/-}$ mice were fertile, although the females showed decreased fertility as described above. However, HSD17B12$^{-/-}$ pups could not be produced, indicating that the null mice died in utero. To study the time of death, HSD17B12-/- embryos were examined at different ages of gestation.

At E7.5 and E8.5, HSD17B12$^{-/-}$ embryos were observed, but the embryos were already significantly retarded at E7.5 compared with the WT or HSD17B12$^{+/-}$ embryos. In HSD171B12$^{+/-}$ embryos, the localization of HSD17B12 expression was detected by β-galactosidase staining, and a low expression level was observed at E7.5 in the embryonic ectoderm and in the yolk sac (Figure 16). In HSD17B12$^{-/-}$ embryos, the boundary between the embryonic and extraembryonic regions was morphologically poorly defined. Further analyses revealed that the null embryos had initiated gastrulation, but the embryonic, and especially the

extraembryonic ectoderm, had not developed normally. Thus, the chorion was not formed, and the allantois was histologically abnormal.

At E8.5, morphological and histological differences between the HSD17B12$^{-/-}$ and WT embryos further increased. Most null embryos lacked somites but had developed the primitive neural tube and headfold. At E8.5, HSD17B12 expression was detected in the neural folds at both anterior and posterior ends and in yolk sac, but the expression was highest in the fore-, mid- and hind brain (Figure 16). Null embryos were significantly smaller that WT embryos and lacked all the normal morphological structures.

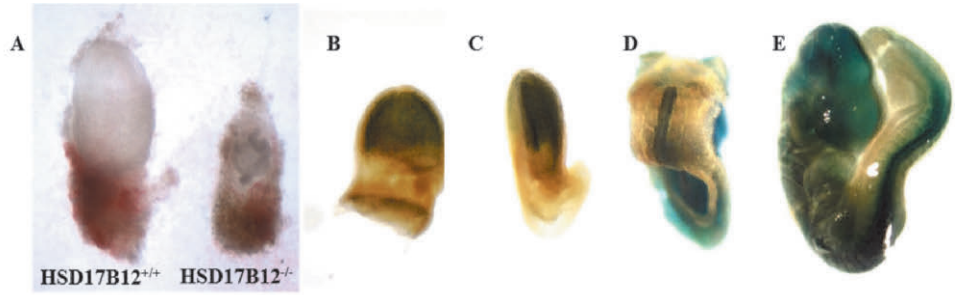

Figure 15. HSD17B12 during early development in mice. A, At E7.5 HSD17B12$^{-/-}$, embryos were already developmentally retarded compared with WT embryos. B and C, At E7.5, HSD17B12 expression was studied with β-galactosidase staining and was localized in embryonic ectoderm in WT embryos (arrowhead). D, At E8.5, HSD17B12 expression was detected in open neural tube. E, At E9.5, the strongest expression was observed in neural tube but also broadly in the whole embryo. *Modified from Rantakari et al. 2010*

At E9.5, HSD17B12$^{-/-}$ embryos could be distinguished from WT embryos based on severe abnormalities in the yolk sack, which did not have any detectable blood vessels. In addition, the null embryos were covered with boll-like structure lacking all normal morphological and histological structures. At E9.5, HSD17B12 expression was detected in the neural tube (Figure 16).

5.2.5 *HSD17B12$^{+/-}$ female mice have no defects in the production of reproductive hormones (II)*

HSD17B12 has been suggested to have a role in the biosynthesis of steroids, and because of the multiple dysfunctions observed in the ovaries, the reproductive

hormone concentrations were measured in the ovaries and serum of WT and HSD17B12$^{+/-}$ mice. All measurements were performed at diestrous. There were no differences in LH, FSH and PRL levels. Furthermore, there were no differences in ovarian concentrations of E1, E2, P4, A-dione or T. In addition, the intraovarian ratios between E1 and E2 or A-dione and T were similar in WT and HSD17B12$^{+/-}$ mice. In agreement with the normal production of estrogen, the uterus wet weight study did not show any differences between WT and HSD17B12$^{+/-}$ females.

5.2.6 *Lack of HSD17B12 leads to disrupted fatty acid synthesis decreasing embryonic growth in vitro (I)*

To study the cell proliferation of HSD17B12$^{-/-}$ embryos, the growth of the ICM of blastocysts was analysed *in vitro*. Blastocysts were collected at E3.5 from HSD17B12$^{+/-}$ matings and cultured separately. Interestingly, the morphology of the knockout blastocysts was normal, indicating that the absence of HSD17B12 does not disturb the preimplantation stage of embryonic development. In 90% of cultures, *null* blastocysts in the ICM did not grow, whereas the ICM failed to grow in 20% of WT and HSD17B12$^{+/-}$ blastocysts. In accordance with these findings, we were unable to isolate null mutated ES cells from blastocysts. FA measurements were performed in isolated WT and HSD17B12$^{+/-}$ ES cells, and interestingly, the level of AA was significantly decreased in HSD17B12$^{+/-}$ ES cells compared with WT cells. LA is obtained from the mother via the placenta, and therefore the level was the same in WT and HSD17B12$^{+/-}$ ES cells.

5.2.7 *HSD17B12$^{+/-}$ ovaries had decreased levels of AA and its downstream eicosanoids (II)*

To study further the role of HSD17B12 in the metabolism of AA and its downstream metabolites, the intraovarian levels of AA, 6-keto $PGF_{1\alpha}$, PGD_2, PGE_2, $PGF_{2\alpha}$, and TXB2 were measured (grey boxes in figure 16). According to the pathway analyses, the concentrations of prostaglandin pathway metabolites were significantly decreased in HSD17B12$^{+/-}$ ovaries (Hotelling's $T2$ test $P>0.005$). Interestingly, there were no chances in the expression of COX1/PTGS1 or COX2/PTGS2 mRNA in ovaries, further indicating that HSD17B12 has a significant role in AA synthesis in mouse ovaries.

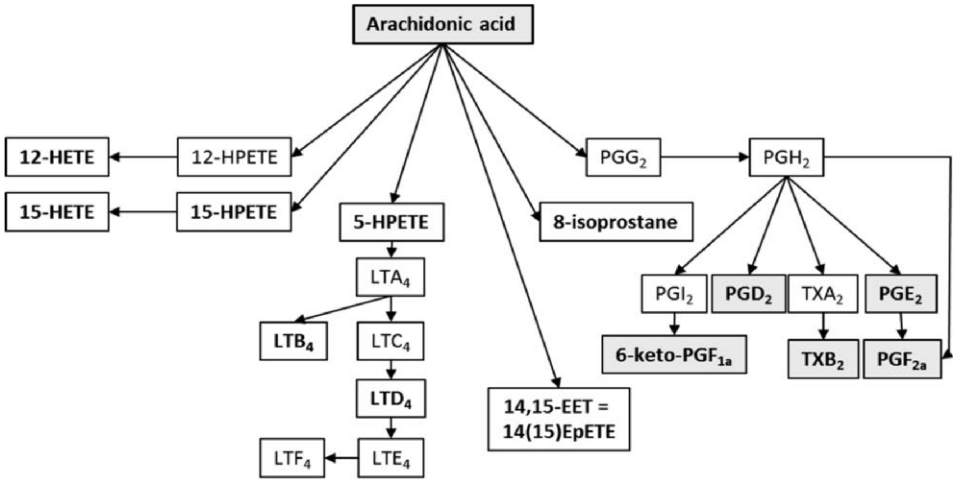

Figure 16. AA and downstream metabolites (12-HPETE: 12-hydroperoxyeicosatetraenoic acid, 12-HETE: 12-hydroxyeicosatetraenoic acid, 15-HPETE: 15-hydroperoxyeicosatetraenoic acid, 15-HETE: 15-hydroxyeicosatetraenoic, 5-HPETE; 5-hydroperoxyeicosatetraenoic acid, LTA_4: leukotriene A4, LTB_4: leukotriene B4, LTC_4: leukotriene C4, LTD_4: leukotriene D4, LTE_4: leukotriene E4, LTF_4: leukotriene F4, 14,15-EET: 14,15-epoxyeicosatrienoic acid, PGG_2: prostaglandin G2, PGH_2: prostaglandin H2, PGI_2: prostaglandin I2, 6-keto $PGF_{1\alpha}$: *6-keto* prostaglandin F1α, PGD_2: prostaglandin D2, TXA_2: thromboxane A2, TXB_2: thromboxane B2, PGE_2: prostaglandin E2 and $PGF_{2\alpha}$: prostaglandin F2α).

5.3 HSD17B12 expression is correlated with prognosis of the ovarian cancer (III)

As shown in the present study, the HSD17B12 enzyme is involved in AA synthesis, and AA and its downstream metabolites have previously been linked to cancer progression. We have also shown that HSD17B12 is broadly expressed in human ovaries. These data motivated us to study further the role of HSD17B12 in ovarian cancer and its co-expression with its upstream and downstream enzymes in the AA pathway, namely, ELOVL5 and COX2, in 144 malignant and 70 benign ovarian lesions.

5.3.1 *ELOVL5, HSD17B12 and COX2 are weakly expressed in benign ovarian lesions (III)*

In mucinous and serous cystadenoma specimens, HSD17B12, COX2 and ELOVL5 enzymes were all expressed in the stroma, whereas only COX2 was also detectable in the epithelium. Moreover, the intensity of HSD17B12 staining varied in the stroma between the samples. In borderline serous cystadenoma, all three enzymes were expressed in the cytoplasm of the epithelium, while varying expression of HSD17B12 was observed in the stroma similar to that observed in serous cystadenoma samples. In addition, the expression of ELOVL5 and COX2 varied more in borderline samples than in serous cystadenoma samples. In summary, all three enzymes were expressed at relatively low levels in all benign ovarian lesions, and their expression was localized in the cytoplasm.

5.3.2 *The expression of HSD17B12, COX2 and ELOVL5 increases as benign serous ovarian lesions progress to higher grade adenocarcinoma (III)*

In serous adenocarcinoma samples, all three enzymes, HSD17B12, COX2 and ELOVL5, were detected in the cytoplasm of the epithelium. The expression levels of all three enzymes increased when the ovarian lesions progressed from benign to malignant stages, although significant differences were only observed within grade two and grade three cancers. The intensity of HSD17B12 staining also increased together with the FIGO stage of the cancer, but not with the cancer grade. Statistically, the difference was significant between FIGO Ia-c and FIGO IIIa-c samples. In contrast, ELOVL5 did not show clear changes in expression levels according to the grade or FIGO stage. However, there was a trend toward a negative correlation between the ELOVL5 intensity and the FIGO stage. COX2 expression increased together with the cancer grade, and the increase was statistically significant between grade one and two or three. Although COX2 expression slightly increased together with the FIGO stage, the increase was not statistically significant.

5.3.3 *The expression levels of HSD17B12, COX2 and ELOVL5 increased with the grade of the endometrial adenocarcinomas, but not in mucinous adenocarcinoma and transitional cell carcinomas (III)*

In endometrioid adenocarcinoma, the expression of all three enzymes, HSD17B12, COX2 and ELOVL5, increased together with the cancer grade, and the staining was localized to the cytoplasm in the epithelium. However, the in-

crease was statistically significant only between grade three and one or two, grade one and two or three, and grade one and three, in the case of HSD17B12, COX2 and ELOVL5, respectively. All enzymes, HSD17B12, COX2 and ELOVL5, showed weak cytoplasmic staining in mucinous adenocarcinoma samples. Although the transition from mucinous cystadenoma to adenocarcinoma significantly increased the expression of all three enzymes, they did not show any changes in expression with an increasing cancer grade or FIGO stage. Transitional cell carcinomas showed a consistently high expression level of HSD17B12 in the cytoplasm of epithelial cells, regardless of the cancer grade. The expression level of ELOVL5 in the epithelial cell cytoplasm was low, and the level varied between samples. Similarly, the COX2 expression level in the cytoplasm of epithelial cells varied highly from very weak to extensively high. In ovarian metastatic carcinoma samples, all enzymes showed a high variation of expression levels between samples. The expression was localized in the cytoplasm of the epithelium, but there was no correlation between the expression level and the cancer grade.

6 DISCUSSION

6.1 HSD17B12 is essential for normal ovarian function and embryonic development

The HSD17B12 enzyme is a member of the HSD17B enzyme family. Although the HSD17B enzymes are involved in steroid metabolism, the main function of the HSD17B12 is still under debate. Some studies indicate that the main role of the enzymes is the conversion of E1 to E2 (Luu-The et al. 2006), but other studies show that the enzyme is involved in FA synthesis (Adamski and Jakob 2001, Mindnich et al. 2004, Saloniemi et al. 2012).

6.1.1 *A decreased level of the HSD17B12 enzyme does not affect steroid levels*

According to our studies, HSD17B12$^{+/-}$ females were subfertile, showing multiple ovarian dysfunctions. Females with only one functional allele had a significantly prolonged estrous cycle, and the diestrous phase was particularly prolonged. In diestrous, the ovary is preparing to start a new cycle or, conversely, waiting for fertilization and pregnancy. In diestrous the CL is the main structure to stabilize the phase, and its correctly timed lysis allows the estrous cycle to continue. In our studies, normal CLs and all follicular stages were observed in HSD17B12$^{+/-}$ ovaries. Interestingly, there were no differences in serum and intraovarian hormone levels in HSD17B12$^{+/-}$ females compared with WT females and the ratio between E1 and E2 was not changed. This finding supports the hypothesis that HSD17B12 does not affect ovarian function by altering the steroid environment, but rather would acts via another pathway, possibly altering local prostaglandin synthesis. In mice, CL remains fully functional until the appearance of the PGF_{2a} signal, originating ipsilateraly from the uterus (Lee et al. 2010). PGF_{2a} initiates the cascades of events in which luteinized cells are decomposed (Figure 8). In contrast, decreased levels of PGF_{2a} lead to an increase in the lifetime of CL, thus prolonging the estrous cycle (Niswender et al. 2000).

6.1.2 *Fully functional HSD17B12 is needed to maintain normal prostaglandin levels in mouse ovaries*

HSD17B12$^{+/-}$ females had significantly lower levels of AA and its downstream metabolites, PGs, in the ovaries. PGs are known to regulate multiple processes in the ovaries, and PGE_2 in particular is needed for follicular maturation, ovulation and the maintenance of meiotic arrest. Conversely, PGF_{2a} is needed for the initiation of luteolysis. HSD17B12$^{+/-}$ females showed several problems in the ovaries, such as polyovular follicles, trapped oocytes and meiotic arrest failure (Figure 17).

Interestingly, COX2-deficient mice have a phenotype similar to HSD17B12$^{+/-}$ females (Lim et al. 1997), such as failed ovulation, fertilization, implantation and decidualization. In contrast, COX1-deficient mice are healthy but have problems in the induction of parturition (Langenbach et al. 1997). COX1 is known to be constitutively expressed, while COX2 is inducible, which may explain the differences between the two mouse models (Lim et al. 1997, Langenbach et al. 1999). COX enzymes are known to be the gatekeepers in prostaglandin production, and PGE2 especially is well known to be important for many normal ovarian functions. PGE2 functions through the G protein-coupled receptor EP2. EP2-deficient mice have a phenotype similar to COX2-deficient mice, with smaller litters and a decreased ovulation rate. Most of the follicles in EP2 null mice did not have normal cumulus cell expansion before ovulation, causing problems in fertilization (Hizaki et al. 1999, Kennedy et al. 1999, Tilley et al. 1999).

Some studies have shown the importance of PGs in ovulation. Gaytán and coworkers (2009) have shown that the inhibition of PGE2 during ovulation prevents follicular wall rupture. The absence of PGs prevents ovulation and leads to a trapped oocyte, i.e., the oocyte stays inside the luteinizing granulosa and theca cells. HSD17B12$^{+/-}$ females showed similar reproductive dysfunctions as COX2$^{-/-}$ mice and EP2$^{-/-}$ mice, supporting our findings and conclusion that *Hsd17b12* regulates female fertility via PGs.

Although the decreased prostaglandin levels could explain many of the HSD17B12$^{+/-}$ female fertility problems, the cause of the formation of polyovular follicles remains unexplained. According to our studies, there were no differences between genotypes in germinal cyst breakdown. Ovaries were studied at PND 3, and no defects were observed in HSD17B12$^{+/-}$ mice. In contrast, we were able to identify one polyovular follicle in one WT ovary, indicating that POFs could also be formed accidentally.

6.1.3 *HSD17B12 regulates meiotic arrest in oocytes*

The most interesting finding in HSD17B12$^{+/-}$ ovaries was the identification of uncontrolled meiotic resumption. In these mice, we could detect a visible meiotic spindle already in secondary follicles and in diestrous. In most cases, we could see the transition to metaphase, but in a few cases even the transition to anaphase was seen.

Normally, meiosis is arrested until the preovulatory peak of LH, which initiates the cascade that allows meiotic resumption (Figure 5) (Handel and Schimenti 2010). This signal is mediated by somatic cells via gap junctions; in follicles, two gap junctions are responsible for transforming the cGMP and cAMP signals. GJA1 (Cx43) is localized between the granulosa cells and GJA4 (Cx37) is localized in the zona pellucida (Richard and Baltz 2014).

Interestingly, according to the whole-genome transcriptome study of HSD17B12$^{+/-}$ ovaries, GJA1 gene expression was downregulated (FC -1.4) and upregulated (FC +1.8). To study the function of GJA4, Simon and co-workers (1997) generated a GJA4-deficient mouse model, and as expected, knockout females were infertile because they were unable to develop antral follicles. Interestingly, the females lacking one allele of the GJA4 gene were completely normal and fertile, indicating that even partially functioning gap junctions are enough for follicular development (Simon et al. 1997). According to these findings, HSD17B12$^{+/-}$ female fertility problems are most likely not caused by the decreased expression of GJA1 and GJA4.

Recent studies have shown that PGE2 also has specific receptors in the oocyte (Kim, Harris and Duffy 2014), as well as in the surrounding somatic cells. Interestingly, Duffy and co-workers (2010) showed that the addition of PGE2 to oocytes *in vitro* decreased the number of maturated oocytes and prevented the resumption of meiosis. They also showed that the level of administered PGE2 was consistent with the measured cAMP level in the oocyte, and changes in cAMP are known to regulate meiotic arrest and resumption. In our studies, HSD17B12$^{+/-}$ ovaries have significantly decreased levels of PGs, and the regulation of meiotic arrest was also disturbed. As previously shown, increased levels of PGE2 inhibit meiotic resumption, and consistently, our findings showed that decreased levels of PGE2 cause premature meiotic resumption (Conti et al. 2012), indicating the need for a delicate balance in the PGE_2 concentration in the ovary.

6.1.4 *Lack of HSD17B12 leads to embryonic lethality*

According to our findings, HSD17B12 is essential for embryonic development and even for ES cell survival, and the absence of the enzyme leads to multiple developmental defects.

The correct balance of FAs is known to be essential during embryonic development; precise levels of AA and DHA especially are needed for neuronal development. Previous studies have shown that deletion of FAS leads to embryonic lethality and that partial deletion of FAS leads to developmental defects (Chirala et al. 2003). Thus, $FAS^{+/-}$ embryos died at various stages of development, and at E9.5, the embryos had not turned and were significantly smaller than normal littermates. According to our results, $HSD17B12^{+/-}$ ES cells had significantly decreased levels of AA, and in blastocyst cultures, $HSD17B12^{-/-}$ blastocysts failed to grow ICM. Furthermore, we were unable to culture $HSD17B12^{-/-}$ES cells. $HSD17B12^{-/-}$ embryos survived longer than $FAS^{-/-}$ embryos, consistent with the observation that FAS is needed for the synthesis of all FAs in the body, whereas HSD17B12 is mainly involved in AA synthesis. Thus, we conclude that the decreased level of AA during early embryonic development is at least one significant cause of the embryonic lethality (Figure 17).

Interestingly, in the whole-genome transcriptome study of $HSD17B12^{+/-}$ ovaries, we observed a significant downregulation of the Pten gene (FC -1.5). Mouse studies have shown that the deletion of Pten causes severe problems in neural tube formation and closure (Bloomekatz et al. 2012). In our studies, HSD17B12 expression was localized at E7.5 in embryonic ectoderm and at E8.5 in neural folds in both regions of body, anterior and posterior. In addition, at E7.5, $HSD17B12^{-/-}$ embryos showed histological abnormalities in both embryonal ectoderm and mesoderm layers. The layers showed an increased cell mass, and the cavities, conversely, were not properly developed. Interestingly, the expression pattern of HSD17B12 was similar to Pten. In addition, Pten-deficient embryos also exhibited deficiencies in mesodermal migration, leading to hypoplasia of the heart. Considered together, HSD17B12 and Pten-deficient mice had similar embryonic defects, including expression localization and morphological defects.

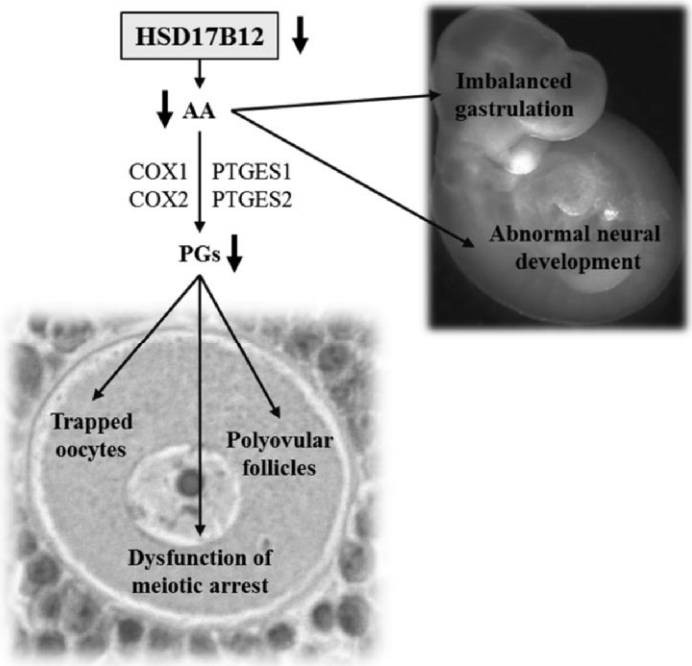

Figure 17. Physiological role of HSD17B12 in early embryonal development and ovarian function.

6.2 HSD17B12 expression increases together with the malignancy of ovarian cancer

HSD17B12 has been shown to be involved in the conversion of E1 to E2, as well as in the synthesis of long-chain FAs, especially AA, a well-known precursor of PGE2 (Moon and Horton 2003, Luu-The et al. 2006). Both of these enzymatic activities are highly relevant in cancer development and progression. According to the present data, HSD17B12 is widely expressed in human ovaries (such as in the theca interna, corpus luteum, granulosa cells, oocytes, and surface epithelium), and studies by others have linked the overexpression of HSD17B12 to a poor prognosis of ovarian cancer, and also to resistance to cisplatin treatment. In addition, *in vitro* studies have shown that silencing HSD17B12 expression with siRNA in cancer cell lines leads to growth inhibition and increases apoptosis (Nagasaki et al. 2009b, Szajnik et al. 2012). Additionally, our data using knockout mice indicated an essential role for the enzyme in cell proliferation during development.

According to our results, HSD17B12 expression increases together with COX2 expression in ovarian serous and endometrioid adenocarcinomas. COX2 is a well-known prognostic factor in ovarian cancer; higher expression levels are linked to a poor prognosis. Conversely, increased expression of HSD17B12 has also been linked to a poor outcome thought to correlate to a poor outcome of patients.

Interestingly, the expression of ELOVL5 was not increased while the ovarian cancer grade increased. ELOVL5 is the partner of HSD17B12 in the synthesis of AA from diet-based LA. Although COX2 and HSD17B12 have been linked to ovarian cancer metabolism, the increase of ELOVL5 expression has mainly been seen in castrate-resistant prostate cancer. Although ELOVL5 synthesizes AA together with HSD17B12 in normal tissue, the expression of these enzymes in cancer is differentially regulated, and the level of ELOVL5 in cancer cells remains relatively stable while the grade and FIGO are increasing. Taken together, the effect of HSD17B12 on ovarian cancer development likely occurs via its involvement in the synthesis of AA and its downstream metabolites.

Interestingly, according to the whole-genome microarray study of the mouse transcriptome from HSD17B12$^{+/-}$ ovaries, a significant upregulation of KISS1, a well-known tumour suppressor gene, was observed. Although this result is from mouse ovaries with downregulated HSD17B12, it provides another theoretical mechanism of enzyme-mediated ovarian cancer progression. Gaytan and co-workers (2009) have shown that the expression of KISS1 is resulted by PGE_2 in normal mouse ovarian tissue. Interestingly, according to clinical studies of ovarian cancer patients, the elevated expression level of KISS1 is negatively correlated with the metastatic activity and poor prognosis (Cao et al. 2016). Other studies have also shown, *in vitro* and *in vivo*, that KISS1 activity suppresses metastatic activity (Jiang et al. 2005). In addition, Jiang and co-workers showed that PKC-α activity is negatively correlated with KISS1 expression in cancer. In addition, in normal ovaries, PKC-α is known to be regulated by PG (Figure 8). According to these findings, the hypothetical pathway is presented in Figure 14, providing another possible mechanism by which HSD17B12 is involved in ovarian cancer progression, in addition to via AA and its downstream metabolites.

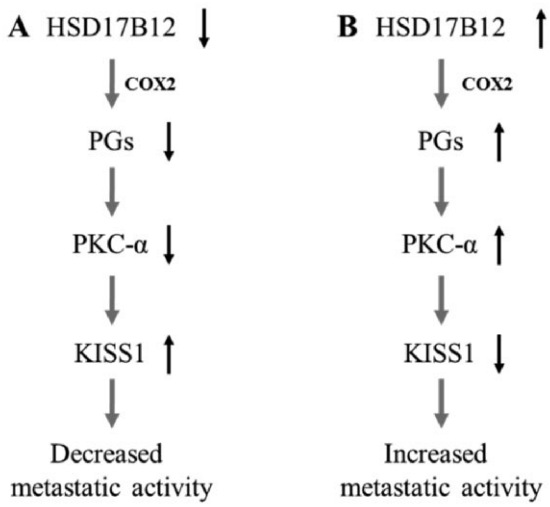

Figure 18. Hypothetical pathway by which HSD17B12 affects the metastatic activity of ovarian cancer. In pathway A, HSD17B12 is downregulated, leading to the upregulation of KISS1 and decreased metastatic activity. Pathway B shows the effect of upregulated HSD17B12, leading to the down-regulation of KISS1 and increasing metastatic activity.

7 CONCLUSIONS

In conclusion, our studies have shown that the HSD17B12 enzyme plays an important role in ovarian function and embryonic development. According to our studies with HSD17B12$^{-/-}$ embryos and ES cells, as well as with HSD17B12+/- females, the enzyme has a significant role in the synthesis of AA and its downstream metabolites. Based on our studies, the main function of the HSD17B12 enzyme is in FA metabolism, namely, AA synthesis, and not in steroid hormone synthesis.

1. HSD17B12 is essential for embryonic development, and the absence of the enzyme leads to abnormal neuronal development, leading to embryonic lethality, mainly because of decreased levels of AA.

2. Fully functional HSD17B12 is needed for normal fertility and ovarian function. Thus, only one functional allele with reduced expression of the protein is not sufficient to maintain normal levels of AA and its downstream metabolites, eicosanoids.

3. HSD17B12 is co-expressed with COX2 in ovarian cancer lesions, and COX2 is known to affect cancer growth via PGs, supporting our hypothesis that HSD17B12 similarly affects ovarian cancer progression via involvement in the production of AA and its downstream metabolites.

ACKNOWLEDGEMENTS

This study was carried out at the Institute of Biomedicine, Research Centre for Integrative Physiology and Pharmacology, University of Turku during the years 2010-2017.

First I wish to thank my supervisors Professor Matti Poutanen, and Docent Leena Strauss. Thank you, Matti for giving me an opportunity to work in your research group. During all these years your support, guidance and trust in this project and me, as well as criticism, have made me the scientist I am now. I cannot thank you, Leena, enough for your encouragement, patience and support during these years. No matter how crazy ideas or plans I had, and despite how busy you were, your door was always open and you found time for me.

Special thanks goes to Pia Rantakari. When I first came to the Department of Physiology as a summer student it was your enthusiasm towards science which had a huge influence to me. Without you and passion in the first place, I most probably would not be here now.

Professor Juha Tapanainen and Assistant professor Andrea Romano are acknowledged for reviewing this thesis and for giving comments and suggestions to make this thesis better. I wish also to thank members of my thesis advisory committee, Professor Kati Elima and Professor Kalervo Hiltunen.

I want to thank all my co-authors Pia Rantakari, Mika Kaimainen, Jukka-Pekka Suomela, Leena Strauss, Kirsi Sainio, Pirjo Pakarinen, Marion Adam, Jenni Mäki-Jouppila, Pauliina Damdimopoulou, Anastasios Damdimopoulos, Juha Kere, Outi Hovatta, Teemu Laajala, Tero Aittokallio, Jerzy Adamski, Henrik Ryberg, Claes Ohlsson, Kaisa Huhtinen, Annika Auranen and Olli Carpén for their valuable collaboration and support during this process.

During these years I have been privileged to have so many wonderful office mates. Last few years I was lucky to get into office B607, and I wish to thank Mari Lehti, Milena Doroszko, Sofia Aakko, Henriette Undeutsch, Tiina Lehtiniemi, Margareeta Mäkelä, Matteo Da Ros, Jenni Mäki-Jouppila and Freja Hartman, and not forgetting my former office mates in C5 floor Heli Jokela, Hanna Heikelä and Heikki Turunen. I wish to thank you all for the discussions and help during these years, you all have made this process doable.

I wish to thank the current and former Professors, Docents, Researchers, Post-docs and students from the Department of Physiology for creating this a great

and supportive environment for all. Thank you Jorma Toppari, Ilpo Huhtaniemi, Noora Kotaja, Marko Kallio, Jukka Kero, Harri Niinimäki, Nafis Rahman, Lauri Pelliniemi, Manuel Tena-Sempere, Pirjo Pakarinen, Marcin Chrusciel, Holger Jäsche, Mirja Nurmio, Annika Adamsson, Christoffer Löf, Juho-Antti Mäkelä, Suvi Ruohonen, Niina Saarinen-Aaltonen, Taija Heinosalo, Petra Sipilä, Helena Virtanen, Fuping Zhang, Adolfo Rivero-Müller, Mahes Tambe, Ashutosh Trehan, Matias Knuuttila, Janne Hakkarainen, Hanna Korhonen, Ram Prakash Yadav, Opeyemi Olotu, Michael Gabriel, Jaakko Koskenniemi, Anna Eggert, Lili Niinimäki, and all the others I may forgot to mention here.

I wish to thank all the lovely people in the Department of Physiology, without your help the day after day work in the lab wold not have been possible. Especially I would like to thank Laboratory Manager Tuula Hämäläinen for taking good care of us and also for making the lab functional place to work. My sincere gratitude goes to Johanna Järvi, Minna Lindroth, Taina Kirjonen, Marko Tirri, Pauliina Toivonen, Katri Hovirinta, Nina Messner, Heli Niittymäki, Heidi Liljenbäck, Mona Niiranen, Jonna Palmu, Erica Nyman, Marja-Riitta Kaajala, Kati Asp, Anu Salminen, Heidi Gerke, Pia Roering, Taija Poikkipuoli, Minna Kangasperko, Leena Karlsson, Merja Leppiaho, Hannele Rekola, Anneli Vesa, and Eila Virransuo.

Suuret kiitokset ystävilleni ja perheelleni kaikesta tuesta näiden vuosien aikana. Erityiskiitos kuuluu aviomiehelleni Teemulle, kiitos että olet jaksanut olla tukenani ja turvanani koko tämän ajan, olet jaksanut muistuttaa siitä mikä elämässä on tärkeintä.

The thesis work was financially supported by Turku Doctoral Programme on Molecular Medicine (TuDMM), Sigrid Juselius Foundation, the Novo Nordisk Foundation and Academy of Finland.

Turku, December 2017

REFERENCES

Ackert, C. L., J. E. Gittens, M. J. O'Brien, J. J. Eppig & G. M. Kidder (2001) Intercellular communication via connexin43 gap junctions is required for ovarian folliculogenesis in the mouse. *Dev Biol,* 233**,** 258-70.

Adamski, J. & F. J. Jakob (2001) A guide to 17beta-hydroxysteroid dehydrogenases. *Mol Cell Endocrinol,* 171**,** 1-4.

Agarwal, R. (2003) The function of COX-2 in human ovarian carcinoma. *Am J Pathol,* 163**,** 368; author reply 368-9.

Agren, J. J., A. Julkunen & I. Penttilä (1992) Rapid separation of serum lipids for fatty acid analysis by a single aminopropyl column. *J Lipid Res,* 33**,** 1871-6.

Ali-Fehmi, R., R. T. Morris, S. Bandyopadhyay, M. Che, V. Schimp, J. M. Malone & A. R. Munkarah (2005) Expression of cyclooxygenase-2 in advanced stage ovarian serous carcinoma: correlation with tumor cell proliferation, apoptosis, angiogenesis, and survival. *Am J Obstet Gynecol,* 192**,** 819-25.

Allaj, V., C. Guo & D. Nie (2013) Non-steroid anti-inflammatory drugs, prostaglandins, and cancer. *Cell Biosci,* 3**,** 8.

Arosh, J. A., S. K. Banu, P. Chapdelaine, E. Madore, J. Sirois & M. A. Fortier (2004) Prostaglandin biosynthesis, transport, and signaling in corpus luteum: a basis for autoregulation of luteal function. *Endocrinology,* 145**,** 2551-60.

Artus, J. & C. Chazaud (2014) A close look at the mammalian blastocyst: epiblast and primitive endoderm formation. *Cell Mol Life Sci,* 71**,** 3327-38.

Artus, J. & M. Cohen-Tannoudji (2008) Cell cycle regulation during early mouse embryogenesis. *Mol Cell Endocrinol,* 282**,** 78-86.

Athanassiadou, P., D. Grapsa, P. Athanassiades, M. Gonidi, A. M. Athanassiadou, A. Tsipis & E. Patsouris (2008) The prognostic significance of COX-2 and survivin expression in ovarian cancer. *Pathol Res Pract,* 204**,** 241-9.

Barnes, N., P. Haywood, P. Flint, W. F. Knox & N. J. Bundred (2006) Survivin expression in in situ and invasive breast cancer relates to COX-2 expression and DCIS recurrence. *Br J Cancer,* 94**,** 253-8.

Behringer, R. R., M. J. Finegold & R. L. Cate (1994) Müllerian-inhibiting substance function during mammalian sexual development. *Cell,* 79**,** 415-25.

Bell, C. E. & A. J. Watson (2013) p38 MAPK regulates cavitation and tight junction function in the mouse blastocyst. *PLoS One,* 8**,** e59528.

Bellemare, V., P. Laberge, S. Noël, A. Tchernof & V. Luu-The (2009) Differential estrogenic 17beta-hydroxysteroid dehydrogenase activity and type 12 17beta-hydroxysteroid dehydrogenase expression levels in preadipocytes and differentiated adipocytes. *J Steroid Biochem Mol Biol,* 114**,** 129-34.

Ben-Ami, I., S. Freimann, L. Armon, A. Dantes, D. Strassburger, S. Friedler, A. Raziel, R. Seger, R. Ron-El & A. Amsterdam (2006) PGE2 up-regulates EGF-like growth factor biosynthesis in human granulosa cells: new insights into the coordination between PGE2 and LH in ovulation. *Mol Hum Reprod,* 12**,** 593-9.

Blanchard, P. G. & V. Luu-The (2007) Differential androgen and estrogen substrates specificity in the mouse and primates type 12 17beta-hydroxysteroid dehydrogenase. *J Endocrinol,* 194**,** 449-55.

Bloomekatz, J., J. Grego-Bessa, I. Migeotte & K. V. Anderson (2012) Pten regulates collective cell migration during specification of the anterior-posterior axis of the mouse embryo. *Dev Biol,* 364**,** 192-201.

Boroviak, T. & J. Nichols (2017) Primate embryogenesis predicts the hallmarks of human naïve pluripotency. *Development,* 144**,** 175-186.

Bristol-Gould, S. K., P. K. Kreeger, C. G. Selkirk, S. M. Kilen, R. W. Cook, J. L. Kipp, L. D. Shea, K. E. Mayo & T. K. Woodruff (2006) Postnatal regulation of germ cells by activin: the establishment of the initial follicle pool. *Dev Biol,* 298**,** 132-48.

Brown, C., J. LaRocca, J. Pietruska, M. Ota, L. Anderson, S. D. Smith, P. Weston, T. Rasoulpour & M. L. Hixon (2010) Subfertility caused by altered follicular development and oocyte growth in female mice lacking PKB alpha/Akt1. *Biol Reprod,* 82**,** 246-56.

Bryja, V., S. Bonilla, L. Cajánek, C. L. Parish, C. M. Schwartz, Y. Luo, M. S. Rao & E. Arenas (2006) An efficient method for the derivation of mouse embryonic stem cells. *Stem Cells,* 24**,** 844-9.

Bézard, J., J. P. Blond, A. Bernard & P. Clouet (1994) The metabolism and availability of essential fatty acids in animal and human tissues. *Reprod Nutr Dev,* 34**,** 539-68.

Cao, F., L. Chen, M. Liu, W. Lin, J. Ji, J. You, F. Qiao & H. Liu (2016) Expression of preoperative KISS1 gene in tumor tissue with epithelial ovarian cancer and its prognostic value. *Medicine (Baltimore),* 95**,** e5296.

Castrillon, D. H., L. Miao, R. Kollipara, J. W. Horner & R. A. DePinho (2003) Suppression of ovarian follicle activation in mice by the transcription factor Foxo3a. *Science,* 301**,** 215-8.

Celik, O., N. Celik, S. Gungor, E. T. Haberal & S. Aydin (2015) Selective Regulation of Oocyte Meiotic Events Enhances Progress in Fertility Preservation Methods. *Biochem Insights,* 8**,** 11-21.

Cha, Y. I., S. H. Kim, D. Sepich, F. G. Buchanan, L. Solnica-Krezel & R. N. DuBois (2006) Cyclooxygenase-1-derived PGE2 promotes cell motility via the G-protein-coupled EP4 receptor during vertebrate gastrulation. *Genes Dev,* 20**,** 77-86.

Chan, A. T., S. Ogino & C. S. Fuchs (2007) Aspirin and the risk of colorectal cancer in relation to the expression of COX-2. *N Engl J Med,* 356**,** 2131-42.

Chandrasekharan, N. V., H. Dai, K. L. Roos, N. K. Evanson, J. Tomsik, T. S. Elton & D. L. Simmons (2002) COX-3, a cyclooxygenase-1 variant inhibited by acetaminophen and other analgesic/antipyretic drugs: cloning, structure, and expression. *Proc Natl Acad Sci U S A,* 99**,** 13926-31.

Chang, H. M., J. Qiao & P. C. Leung (2016) Oocyte-somatic cell interactions in the human ovary-novel role of bone morphogenetic proteins and growth differentiation factors. *Hum Reprod Update,* 23**,** 1-18.

Chazaud, C., Y. Yamanaka, T. Pawson & J. Rossant (2006) Early lineage segregation between epiblast and primitive endoderm in mouse blastocysts through the Grb2-MAPK pathway. *Dev Cell,* 10**,** 615-24.

Chirala, S. S., H. Chang, M. Matzuk, L. Abu-Elheiga, J. Mao, K. Mahon, M. Finegold & S. J. Wakil (2003) Fatty acid synthesis is essential in embryonic development: fatty acid synthase null mutants and most of the heterozygotes die in utero. *Proc Natl Acad Sci U S A,* 100**,** 6358-63.

Clift, D. & M. Schuh (2013) Restarting life: fertilization and the transition from meiosis to mitosis. *Nat Rev Mol Cell Biol,* 14**,** 549-62.

Conti, M., C. B. Andersen, F. Richard, C. Mehats, S. Y. Chun, K. Horner, C. Jin & A. Tsafriri (2002) Role of cyclic nucleotide signaling in oocyte maturation. *Mol Cell Endocrinol,* 187**,** 153-9.

Conti, M., C. B. Andersen, F. J. Richard, K. Shitsukawa & A. Tsafriri (1998) Role of cyclic nucleotide phosphodiesterases in resumption of meiosis. *Mol Cell Endocrinol,* 145**,** 9-14.

Conti, M., M. Hsieh, A. M. Zamah & J. S. Oh (2012) Novel signaling mechanisms in the ovary during oocyte maturation and ovulation. *Mol Cell Endocrinol,* 356**,** 65-73.

Creuzet, S. E., S. Martinez & N. M. Le Douarin (2006) The cephalic neural crest exerts a critical effect on forebrain and midbrain development. *Proc Natl Acad Sci U S A,* 103**,** 14033-8.

Crofford, L. J. (1997) COX-1 and COX-2 tissue expression: implications and predictions. *J Rheumatol Suppl,* 49**,** 15-9.

Dard, N., M. Breuer, B. Maro & S. Louvet-Vallée (2008) Morphogenesis of the mammalian blastocyst. *Mol Cell Endocrinol,* 282**,** 70-7.

Day, J. M., P. A. Foster, H. J. Tutill, M. F. Parsons, S. P. Newman, S. K. Chander, G. M. Allan, H. R. Lawrence, N. Vicker, B. V. Potter, M. J. Reed & A. Purohit (2008) 17beta-hydroxysteroid dehydrogenase Type 1, and not Type 12, is a target for endocrine therapy of hormone-dependent breast cancer. *Int J Cancer,* 122**,** 1931-40.

Di Cristofano, A., B. Pesce, C. Cordon-Cardo & P. P. Pandolfi (1998) Pten is essential for embryonic development and tumour suppression. *Nat Genet,* 19**,** 348-55.

Diaz, F. J., K. Wigglesworth & J. J. Eppig (2007) Oocytes determine cumulus cell lineage in mouse ovarian follicles. *J Cell Sci,* 120**,** 1330-40.

Ding, W., W. Wang, B. Zhou, W. Zhang, P. Huang, F. Shi & K. Taya (2010) Formation of primordial follicles and immunolocalization of PTEN, PKB and FOXO3A proteins in the ovaries of fetal and neonatal pigs. *J Reprod Dev,* 56**,** 162-8.

Downey, B. R., J. E. Mootoo & S. E. Doyle (1998) A role for lipoxygenase metabolites of arachidonic acid in porcine ovulation. *Anim Reprod Sci,* 49**,** 269-79.

Downs, K. M. (2002) Early placental ontogeny in the mouse. *Placenta,* 23**,** 116-31.

Downs, S. M. (2010) Regulation of the G2/M transition in rodent oocytes. *Mol Reprod Dev,* 77**,** 566-85.

Dozier, B. L., K. Watanabe & D. M. Duffy (2008) Two pathways for prostaglandin F2 alpha synthesis by the primate periovulatory follicle. *Reproduction,* 136**,** 53-63.

Duffy, D. M. (2015) Novel contraceptive targets to inhibit ovulation: the prostaglandin E2 pathway. *Hum Reprod Update,* 21**,** 652-70.

Duncan, F. E., S. B. Moss & C. J. Williams (2006) Knockdown of the cAMP-dependent protein kinase (PKA) Type Ialpha regulatory subunit in mouse oocytes disrupts meiotic arrest and results in meiotic spindle defects. *Dev Dyn,* 235**,** 2961-8.

Durlinger, A. L., M. J. Gruijters, P. Kramer, B. Karels, H. A. Ingraham, M. W. Nachtigal, J. T. Uilenbroek, J. A. Grootegoed & A. P. Themmen (2002) Anti-Müllerian Hormone Inhibits Initiation of Primordial Follicle Growth in the Mouse Ovary. *Endocrinology,* 143**,** 1076-1084.

Durlinger, A. L., P. Kramer, B. Karels, F. H. de Jong, J. T. Uilenbroek, J. A. Grootegoed & A. P. Themmen (1999) Control of primordial follicle recruitment by anti-Müllerian hormone in the mouse ovary. *Endocrinology,* 140**,** 5789-96.

Entchev, E. V., D. Schwudke, V. Zagoriy, V. Matyash, A. Bogdanova, B. Habermann, L. Zhu, A. Shevchenko & T. V. Kurzchalia (2008) LET-767 is required for the production of branched chain and long chain fatty acids in Caenorhabditis elegans. *J Biol Chem,* 283**,** 17550-60.

Eppig, J. J. (2001) Oocyte control of ovarian follicular development and function in mammals. *Reproduction,* 122**,** 829-38.

Eppig, J. J., K. Wigglesworth & F. L. Pendola (2002) The mammalian oocyte orchestrates the rate of ovarian follicular development. *Proc Natl Acad Sci U S A,* 99**,** 2890-4.

Erez, N. (2015) Cancer: Opening LOX to metastasis. *Nature,* 522**,** 41-2.

Ezin, A. M., S. E. Fraser & M. Bronner-Fraser (2009) Fate map and morphogenesis of presumptive neural crest and dorsal neural tube. *Dev Biol,* 330**,** 221-36.

Fehring, R. J., M. Schneider & K. Raviele (2006) Variability in the phases of the menstrual cycle. *J Obstet Gynecol Neonatal Nurs,* 35**,** 376-84.

Fernandois, D., G. Cruz, E. K. Na, H. E. Lara & A. H. Paredes (2017) Kisspeptin level in the aging ovary is regulated by the sympathetic nervous system. *J Endocrinol,* 232**,** 97-105.

FOLCH, J., M. LEES & G. H. SLOANE STANLEY (1957) A simple method for the isolation and purification of total lipides from animal tissues. *J Biol Chem,* 226**,** 497-509.

Funk, C. D. (2001) Prostaglandins and leukotrienes: advances in eicosanoid biology. *Science,* 294**,** 1871-5.

Gamage, T. K., L. W. Chamley & J. L. James (2016) Stem cell insights into human trophoblast lineage differentiation. *Hum Reprod Update,* 23**,** 77-103.

Gaytán, F., C. Bellido, M. Gaytán, C. Morales & J. E. Sánchez-Criado (2003) Differential effects of RU486 and indomethacin on follicle rupture during the ovulatory process in the rat. *Biol Reprod,* 69**,** 99-105.

Gaytán, F., M. Gaytán, J. M. Castellano, M. Romero, J. Roa, B. Aparicio, N. Garrido, J. E. Sánchez-Criado, R. P. Millar, A. Pellicer, H. M. Fraser & M. Tena-Sempere (2009) KiSS-1 in the mammalian ovary: distribution of kisspeptin in human and marmoset and alterations in KiSS-1 mRNA levels in a rat model of ovulatory dysfunction. *Am J Physiol Endocrinol Metab,* 296**,** E520-31.

Grego-Bessa, J., J. Bloomekatz, P. Castel, T. Omelchenko, J. Baselga & K. V. Anderson (2016) The tumor suppressor PTEN and the PDK1 kinase regulate formation of the columnar neural epithelium. *Elife,* 5**,** e12034.

Grive, K. J. & R. N. Freiman (2015) The developmental origins of the mammalian ovarian reserve. *Development,* 142**,** 2554-63.

Grive, K. J., E. A. Gustafson, K. A. Seymour, M. Baddoo, C. Schorl, K. Golnoski, A. Rajkovic, A. S. Brodsky & R. N. Freiman (2016) TAF4b Regulates Oocyte-Specific Genes Essential for Meiosis. *PLoS Genet,* 12**,** e1006128.

Haavisto, A. M., K. Pettersson, M. Bergendahl, A. Perheentupa, J. F. Roser & I. Huhtaniemi (1993) A supersensitive immunofluorometric assay for rat luteinizing hormone. *Endocrinology,* 132**,** 1687-91.

Handel, M. A. & J. C. Schimenti (2010) Genetics of mammalian meiosis: regulation, dynamics and impact on fertility. *Nat Rev Genet,* 11**,** 124-36.

Hasegawa, K., Y. Ohashi, K. Ishikawa, A. Yasue, R. Kato, Y. Achiwa, E. Nishio & Y. Udagawa (2005) Expression of cyclooxygenase-2 in uterine endometrial cancer and anti-tumor effects of a selective COX-2 inhibitor. *Int J Oncol,* 26**,** 1419-28.

Heinz, S., C. Benner, N. Spann, E. Bertolino, Y. C. Lin, P. Laslo, J. X. Cheng, C. Murre, H. Singh & C. K. Glass (2010) Simple combinations of lineage-determining transcription factors prime cis-regulatory elements required for macrophage and B cell identities. *Mol Cell,* 38**,** 576-89.

Hizaki, H., E. Segi, Y. Sugimoto, M. Hirose, T. Saji, F. Ushikubi, T. Matsuoka, Y. Noda, T. Tanaka, N. Yoshida, S. Narumiya & A. Ichikawa (1999) Abortive expansion of the cumulus and impaired fertility in mice lacking the prostaglandin E receptor subtype EP(2). *Proc Natl Acad Sci U S A,* 96**,** 10501-6.

Huang, Y., K. Hua, X. Zhou, H. Jin, X. Chen, X. Lu, Y. Yu, X. Zha & Y. Feng (2008) Activation of the PI3K/AKT pathway mediates FSH-stimulated VEGF expression in ovarian serous cystadenocarcinoma. *Cell Res,* 18**,** 780-91.

Hussein, T. S., J. G. Thompson & R. B. Gilchrist (2006) Oocyte-secreted factors enhance oocyte developmental competence. *Dev Biol,* 296**,** 514-21.

Hyde, C. A. & S. Missailidis (2009) Inhibition of arachidonic acid metabolism and its implication on cell proliferation and tumour-angiogenesis. *Int Immunopharmacol,* 9**,** 701-15.

Jayakumar, A., S. S. Chirala & S. J. Wakil (1997) Human fatty acid synthase: assembling recombinant halves of the fatty acid synthase subunit protein reconstitutes enzyme activity. *Proc Natl Acad Sci U S A,* 94**,** 12326-30.

Jiang, Y., M. Berk, L. S. Singh, H. Tan, L. Yin, C. T. Powell & Y. Xu (2005) KiSS1 suppresses metastasis in human ovarian cancer via inhibition of protein kinase C alpha. *Clin Exp Metastasis,* 22**,** 369-76.

John, G. B., T. D. Gallardo, L. J. Shirley & D. H. Castrillon (2008) Foxo3 is a PI3K-dependent molecular switch controlling the initiation of oocyte growth. *Dev Biol,* 321**,** 197-204.

John, G. B., L. J. Shirley, T. D. Gallardo & D. H. Castrillon (2007) Specificity of the requirement for Foxo3 in primordial follicle activation. *Reproduction,* 133**,** 855-63.

Joyce, I. M., A. T. Clark, F. L. Pendola & J. J. Eppig (2000) Comparison of recombinant growth differentiation factor-9 and oocyte regulation of KIT ligand messenger ribonucleic acid expression in mouse ovarian follicles. *Biol Reprod,* 63**,** 1669-75.

Juengel, J. L., J. D. Haworth, M. K. Rollyson, P. J. Silva, H. R. Sawyer & G. D. Niswender (2000) Effect of dose of prostaglandin F(2alpha) on steroidogenic components and oligonucleosomes in ovine luteal tissue. *Biol Reprod,* 62**,** 1047-51.

Jump, D. B. (2009) Mammalian fatty acid elongases. *Methods Mol Biol,* 579**,** 375-89.

Kennedy, C. R., Y. Zhang, S. Brandon, Y. Guan, K. Coffee, C. D. Funk, M. A. Magnuson, J. A. Oates, M. D. Breyer & R. M. Breyer (1999) Salt-sensitive hypertension and reduced fertility in mice lacking the prostaglandin EP2 receptor. *Nat Med,* 5**,** 217-20.

Khor, L. Y., K. Bae, A. Pollack, M. E. Hammond, D. J. Grignon, V. M. Venkatesan, S. A. Rosenthal, M. A. Ritter, H. M. Sandler, G. E. Hanks, W. U. Shipley & A. P. Dicker (2007) COX-2 expression predicts prostate-cancer outcome: analysis of data from the RTOG 92-02 trial. *Lancet Oncol,* 8**,** 912-20.

Kidder, G. M. & B. C. Vanderhyden (2010) Bidirectional communication between oocytes and follicle cells: ensuring oocyte developmental competence. *Can J Physiol Pharmacol,* 88**,** 399-413.

Kim, D., G. Pertea, C. Trapnell, H. Pimentel, R. Kelley & S. L. Salzberg (2013) TopHat2: accurate alignment of transcriptomes in the presence of insertions, deletions and gene fusions. *Genome Biol,* 14**,** R36.

Kim, S. O., S. M. Harris & D. M. Duffy (2014) Prostaglandin E2 (EP) receptors mediate PGE2-specific events in ovulation and luteinization within primate ovarian follicles. *Endocrinology,* 155**,** 1466-75.

Kino, Y., F. Kojima, K. Kiguchi, R. Igarashi, B. Ishizuka & S. Kawai (2005) Prostaglandin E2 production in ovarian cancer cell lines is regulated by cyclooxygenase-1, not cyclooxygenase-2. *Prostaglandins Leukot Essent Fatty Acids,* 73**,** 103-11.

Krol, E., S. A. Martin, I. T. Huhtaniemi, A. Douglas & J. R. Speakman. 2011. Negative correlation between milk production and brown adipose tissue gene expression in lactating mice. In *J Exp Biol*, 4160-70. England.

Krysan, K., H. Dalwadi, S. Sharma, M. Põld & S. Dubinett (2004) Cyclooxygenase 2-dependent expression of survivin is critical for apoptosis resistance in non-small cell lung cancer. *Cancer Res,* 64**,** 6359-62.

Kumar, P. & S. F. Sait (2011) Luteinizing hormone and its dilemma in ovulation induction. *J Hum Reprod Sci,* 4**,** 2-7.

Kumar, T. R., Y. Wang, N. Lu & M. M. Matzuk (1997) Follicle stimulating hormone is required for ovarian follicle maturation but not male fertility. *Nat Genet,* 15**,** 201-4.

Langenbach, R., C. D. Loftin, C. Lee & H. Tiano (1999) Cyclooxygenase-deficient mice. A summary of their characteristics and susceptibilities to inflammation and carcinogenesis. *Ann N Y Acad Sci,* 889**,** 52-61.

Langenbach, R., S. G. Morham, H. F. Tiano, C. D. Loftin, B. I. Ghanayem, P. C. Chulada, J. F. Mahler, B. J. Davis & C. A. Lee (1997) Disruption of the mouse cyclooxygenase 1 gene. Characteristics of the mutant and areas of future study. *Adv Exp Med Biol,* 407**,** 87-92.

Langmead, B. & S. L. Salzberg (2012) Fast gapped-read alignment with Bowtie 2. *Nat Methods,* 9**,** 357-9.

Lee, J., J. A. McCracken, S. K. Banu, R. Rodriguez, T. K. Nithy & J. A. Arosh (2010) Transport of prostaglandin F(2alpha) pulses from the uterus to the ovary at the time of luteolysis in ruminants is regulated by prostaglandin transporter-mediated mechanisms. *Endocrinology,* 151**,** 3326-35.

Lee, J. Y., S. K. Myung & Y. S. Song (2013) Prognostic role of cyclooxygenase-2 in epithelial ovarian cancer: a meta-analysis of observational studies. *Gynecol Oncol,* 129**,** 613-9.

Levine, J. E., A. C. Bauer-Dantoin, L. M. Besecke, L. A. Conaghan, S. J. Legan, J. M. Meredith, F. J. Strobl, J. H. Urban, K. M. Vogelsong & A. M. Wolfe (1991) Neuroendocrine regulation of the luteinizing hormone-releasing hormone pulse generator in the rat. *Recent Prog Horm Res,* 47**,** 97-151; discussion 151-3.

Light, A. & S. R. Hammes (2015) LH-Induced Steroidogenesis in the Mouse Ovary, but Not Testis, Requires Matrix Metalloproteinase 2- and 9-Mediated Cleavage of Upregulated EGF Receptor Ligands. *Biol Reprod,* 93**,** 65.

Lim, H., B. C. Paria, S. K. Das, J. E. Dinchuk, R. Langenbach, J. M. Trzaskos & S. K. Dey (1997) Multiple female reproductive failures in cyclooxygenase 2-deficient mice. *Cell,* 91**,** 197-208.

Liu, B., Y. Wang, K. L. Fillgrove & V. E. Anderson (2002) Triclosan inhibits enoyl-reductase of type I fatty acid synthase in vitro and is cytotoxic to MCF-7 and SKBr-3 breast cancer cells. *Cancer Chemother Pharmacol,* 49**,** 187-93.

Liu, K., S. Rajareddy, L. Liu, K. Jagarlamudi, K. Boman, G. Selstam & P. Reddy (2006) Control of mammalian oocyte growth and early follicular development by the oocyte PI3 kinase pathway: new roles for an old timer. *Dev Biol,* 299**,** 1-11.

Liu, L., N. Kong, G. Xia & M. Zhang (2013) Molecular control of oocyte meiotic arrest and resumption. *Reprod Fertil Dev,* 25**,** 463-71.

Loftus, T. M., D. E. Jaworsky, G. L. Frehywot, C. A. Townsend, G. V. Ronnett, M. D. Lane & F. P. Kuhajda (2000) Reduced food intake and body weight in mice treated with fatty acid synthase inhibitors. *Science,* 288**,** 2379-81.

Lu, S. & M. C. Archer (2005) Fatty acid synthase is a potential molecular target for the chemoprevention of breast cancer. *Carcinogenesis,* 26**,** 153-7.

Lukacik, P., K. L. Kavanagh & U. Oppermann (2006) Structure and function of human 17beta-hydroxysteroid dehydrogenases. *Mol Cell Endocrinol,* 248**,** 61-71.

Luu-The, V., P. Tremblay & F. Labrie (2006) Characterization of type 12 17beta-hydroxysteroid dehydrogenase, an isoform of type 3 17beta-hydroxysteroid dehydrogenase responsible for estradiol formation in women. *Mol Endocrinol,* 20**,** 437-43.

Magoffin, D. A. (2005) Ovarian theca cell. *Int J Biochem Cell Biol,* 37**,** 1344-9.

Makker, A., M. M. Goel & A. A. Mahdi (2014) PI3K/PTEN/Akt and TSC/mTOR signaling pathways, ovarian dysfunction, and infertility: an update. *J Mol Endocrinol,* 53**,** R103-18.

Mamsen, L. S., C. B. Brøchner, A. G. Byskov & K. Møllgard (2012) The migration and loss of human primordial germ stem cells from the hind gut epithelium towards the gonadal ridge. *Int J Dev Biol,* 56**,** 771-8.

Marikawa, Y. & V. B. Alarcón (2009) Establishment of trophectoderm and inner cell mass lineages in the mouse embryo. *Mol Reprod Dev,* 76**,** 1019-32.

Markovič, T., Ž. Jakopin, M. S. Dolenc & I. Mlinarič-Raščan (2017) Structural features of subtype-selective EP receptor modulators. *Drug Discov Today,* 22**,** 57-71.

Marston, A. L. & A. Amon (2004) Meiosis: cell-cycle controls shuffle and deal. *Nat Rev Mol Cell Biol,* 5**,** 983-97.

Matzuk, M. M., K. H. Burns, M. M. Viveiros & J. J. Eppig (2002) Intercellular communication in the mammalian ovary: oocytes carry the conversation. *Science,* 296**,** 2178-80.

Menter, D. G. & R. N. Dubois (2012) Prostaglandins in cancer cell adhesion, migration, and invasion. *Int J Cell Biol,* 2012**,** 723419.

Mikuni, M., M. Pall, C. M. Peterson, C. A. Peterson, P. Hellberg, M. Brännström, J. S. Richards & L. Hedin (1998) The selective prostaglandin endoperoxide synthase-2 inhibitor, NS-398, reduces prostaglandin production and ovulation in vivo and in vitro in the rat. *Biol Reprod,* 59**,** 1077-83.

Miller, B. H. & J. S. Takahashi (2013) Central circadian control of female reproductive function. *Front Endocrinol (Lausanne),* 4**,** 195.

Mindnich, R., M. Hrabe de Angelis & J. Adamski (2007) Functional genome analysis indicates loss of 17beta-hydroxysteroid dehydrogenase type 2 enzyme in the zebrafish. *J Steroid Biochem Mol Biol,* 103**,** 35-43.

Mindnich, R., G. Möller & J. Adamski (2004) The role of 17 beta-hydroxysteroid dehydrogenases. *Mol Cell Endocrinol,* 218**,** 7-20.

Monniaux, D. (2016) Driving folliculogenesis by the oocyte-somatic cell dialog: Lessons from genetic models. *Theriogenology,* 86**,** 41-53.

Moon, Y. A., R. E. Hammer & J. D. Horton (2009) Deletion of ELOVL5 leads to fatty liver through activation of SREBP-1c in mice. *J Lipid Res,* 50**,** 412-23.

Moon, Y. A. & J. D. Horton (2003) Identification of two mammalian reductases involved in the two-carbon fatty acyl elongation cascade. *J Biol Chem,* 278**,** 7335-43.

Moore, R. K., G. F. Erickson & S. Shimasaki (2004) Are BMP-15 and GDF-9 primary determinants of ovulation quota in mammals? *Trends Endocrinol Metab,* 15**,** 356-61.

Moreno, J. J. (2009) New aspects of the role of hydroxyeicosatetraenoic acids in cell growth and cancer development. *Biochem Pharmacol,* 77**,** 1-10.

Morrison, W. R. & L. M. Smith (1964) preparation of fatty acid methyl esters and dimethylacetals from lipids with boron fluoride--methanol. *J Lipid Res,* 5**,** 600-8.

Nagasaki, S., Y. Miki, J. Akahira, T. Suzuki & H. Sasano (2009a) Transcriptional regulation of 17beta-hydroxysteroid dehydrogenase type 12 by SREBP-1. *Mol Cell Endocrinol,* 307**,** 163-8.

Nagasaki, S., T. Suzuki, Y. Miki, J. Akahira, K. Kitada, T. Ishida, H. Handa, N. Ohuchi & H. Sasano (2009b) 17Beta-hydroxysteroid dehydrogenase type 12 in human breast carcinoma: a prognostic factor via potential regulation of fatty acid synthesis. *Cancer Res,* 69**,** 1392-9.

Narumiya, S. (2007) Physiology and pathophysiology of prostanoid receptors. *Proc Jpn Acad Ser B Phys Biol Sci,* 83**,** 296-319.

Narumiya, S., Y. Sugimoto & F. Ushikubi (1999) Prostanoid receptors: structures, properties, and functions. *Physiol Rev,* 79**,** 1193-226.

Nautiyal, J., J. H. Steel, M. M. Rosell, E. Nikolopoulou, K. Lee, F. J. Demayo, R. White, J. S. Richards & M. G. Parker (2010) The nuclear receptor cofactor receptor-interacting protein 140 is a positive regulator of amphiregulin expression and cumulus cell-oocyte complex expansion in the mouse ovary. *Endocrinology,* 151**,** 2923-32.

Nelson, S. E., M. P. McLean, P. G. Jayatilak & G. Gibori (1992) Isolation, characterization, and culture of cell subpopulations forming the pregnant rat corpus luteum. *Endocrinology,* 130**,** 954-66.

Nguyen, M., T. Camenisch, J. N. Snouwaert, E. Hicks, T. M. Coffman, P. A. Anderson, N. N. Malouf & B. H. Koller (1997) The prostaglandin receptor EP4 triggers remodelling of the cardiovascular system at birth. *Nature,* 390**,** 78-81.

Nilsson, M. E., L. Vandenput, Å. Tivesten, A. K. Norlén, M. K. Lagerquist, S. H. Windahl, A. E. Börjesson, H. H. Farman, M. Poutanen, A. Benrick, M. Maliqueo, E. Stener-Victorin, H. Ryberg & C. Ohlsson (2015) Measurement of a Comprehensive Sex Steroid Profile in Rodent Serum by High-Sensitive Gas Chromatography-Tandem Mass Spectrometry. *Endocrinology,* 156**,** 2492-502.

Niswender, G. D., J. L. Juengel, P. J. Silva, M. K. Rollyson & E. W. McIntush (2000) Mechanisms controlling the function and life span of the corpus luteum. *Physiol Rev,* 80**,** 1-29.

Ochsner, S. A., D. L. Russell, A. J. Day, R. M. Breyer & J. S. Richards (2003) Decreased expression of tumor necrosis factor-alpha-stimulated gene 6 in cumulus cells of the cyclooxygenase-2 and EP2 null mice. *Endocrinology,* 144**,** 1008-19.

Ohno, Y., S. Suto, M. Yamanaka, Y. Mizutani, S. Mitsutake, Y. Igarashi, T. Sassa & A. Kihara (2010) ELOVL1 production of C24 acyl-CoAs is linked to C24 sphingolipid synthesis. *Proc Natl Acad Sci U S A,* 107**,** 18439-44.

Olofsson, J. & P. C. Leung (1994) Auto/paracrine role of prostaglandins in corpus luteum function. *Mol Cell Endocrinol,* 100**,** 87-91.

Otsuka, F., K. J. McTavish & S. Shimasaki (2011) Integral role of GDF-9 and BMP-15 in ovarian function. *Mol Reprod Dev,* 78**,** 9-21.

Panigrahy, D., A. Kaipainen, E. R. Greene & S. Huang (2010) Cytochrome P450-derived eicosanoids: the neglected pathway in cancer. *Cancer Metastasis Rev,* 29**,** 723-35.

Pepling, M. E. (2012) Follicular assembly: mechanisms of action. *Reproduction,* 143**,** 139-49.

Picton, H. M. (2001) Activation of follicle development: the primordial follicle. *Theriogenology,* 55**,** 1193-210.

Plourde, M., A. Ferland, P. Soucy, Y. Hamdi, M. Tranchant, F. Durocher, O. Sinilnikova, V. Luu The, J. Simard & I. BRCAs (2009) Analysis of 17beta-hydroxysteroid dehydrogenase types 5, 7, and 12 genetic sequence variants in breast cancer cases from French Canadian Families with high risk of breast and ovarian cancer. *J Steroid Biochem Mol Biol,* 116**,** 134-53.

Qiu, X., J. C. Cheng, H. M. Chang & P. C. Leung (2014) COX2 and PGE2 mediate EGF-induced E-cadherin-independent human ovarian cancer cell invasion. *Endocr Relat Cancer,* 21**,** 533-43.

Raju, G. A., R. Chavan, M. Deenadayal, D. Gunasheela, R. Gutgutia, G. Haripriya, M. Govindarajan, N. H. Patel & A. S. Patki (2013) Luteinizing hormone and follicle stimulating hormone synergy: A review of role in controlled ovarian hyper-stimulation. *J Hum Reprod Sci,* 6**,** 227-34.

Reddy, P., L. Liu, D. Adhikari, K. Jagarlamudi, S. Rajareddy, Y. Shen, C. Du, W. Tang, T. Hämäläinen, S. L. Peng, Z. J. Lan, A. J. Cooney, I. Huhtaniemi & K. Liu (2008) Oocyte-specific deletion of Pten causes premature activation of the primordial follicle pool. *Science,* 319**,** 611-3.

Rich, T. C., W. Xin, C. Mehats, K. A. Hassell, L. A. Piggott, X. Le, J. W. Karpen & M. Conti (2007) Cellular mechanisms underlying prostaglandin-induced transient cAMP signals near the plasma membrane of HEK-293 cells. *Am J Physiol Cell Physiol,* 292**,** C319-31.

Richard, S. & J. M. Baltz (2014) Prophase I arrest of mouse oocytes mediated by natriuretic peptide precursor C requires GJA1 (connexin-43) and GJA4 (connexin-37) gap junctions in the antral follicle and cumulus-oocyte complex. *Biol Reprod,* 90**,** 137.

Rouzer, C. A. & L. J. Marnett (2009) Cyclooxygenases: structural and functional insights. *J Lipid Res,* 50 Suppl**,** S29-34.

Sagana, R. L., M. Yan, A. M. Cornett, J. L. Tsui, D. A. Stephenson, S. K. Huang, B. B. Moore, M. N. Ballinger, J. Melonakos, C. D. Kontos, D. M. Aronoff, M. Peters-Golden & E. S. White (2009) Phosphatase and tensin homologue on chromosome 10 (PTEN) directs prostaglandin E2-mediated fibroblast responses via regulation of E prostanoid 2 receptor expression. *J Biol Chem,* 284**,** 32264-71.

Sakamoto, K., K. Miwa, T. Ezashi, E. Okuda-Ashitaka, K. Okuda, T. Houtani, T. Sugimoto, S. Ito & O. Hayaishi (1995) Expression of mRNA encoding the prostaglandin F2 alpha receptor in bovine corpora lutea throughout the oestrous cycle and pregnancy. *J Reprod Fertil,* 103**,** 99-105.

Sakurai, N., Y. Miki, T. Suzuki, K. Watanabe, T. Narita, K. Ando, T. M. Yung, D. Aoki, H. Sasano & H. Handa (2006) Systemic distribution and tissue localizations of human 17beta-hydroxysteroid dehydrogenase type 12. *J Steroid Biochem Mol Biol,* 99**,** 174-81.

Saloniemi, T., H. Jokela, L. Strauss, P. Pakarinen & M. Poutanen (2012) The diversity of sex steroid action: novel functions of hydroxysteroid (17β) dehydrogenases as revealed by genetically modified mouse models. *J Endocrinol,* 212**,** 27-40.

Sato, J., M. Nasu & M. Tsuchitani (2016) Comparative histopathology of the estrous or menstrual cycle in laboratory animals. *J Toxicol Pathol,* 29**,** 155-62.

Schneider, C. & A. Pozzi (2011) Cyclooxygenases and lipoxygenases in cancer. *Cancer Metastasis Rev,* 30**,** 277-94.

Segi, E., Y. Sugimoto, A. Yamasaki, Y. Aze, H. Oida, T. Nishimura, T. Murata, T. Matsuoka, F. Ushikubi, M. Hirose, T. Tanaka, N. Yoshida, S. Narumiya & A. Ichikawa (1998) Patent ductus arteriosus and neonatal death in prostaglandin receptor EP4-deficient mice. *Biochem Biophys Res Commun,* 246**,** 7-12.

Sherman, B. M. & S. G. Korenman (1975) Hormonal characteristics of the human menstrual cycle throughout reproductive life. *J Clin Invest,* 55**,** 699-706.

Shi, L., L. H. Reid, W. D. Jones, R. Shippy, J. A. Warrington, S. C. Baker, P. J. Collins, F. de Longueville, E. S. Kawasaki, K. Y. Lee, Y. Luo, Y. A. Sun, J. C. Willey, R. A. Setterquist, G. M. Fischer, W. Tong, Y. P. Dragan, D. J. Dix, F. W. Frueh, F. M. Goodsaid, D. Herman, R. V. Jensen, C. D. Johnson, E. K. Lobenhofer, R. K. Puri, U. Schrf, J. Thierry-Mieg, C. Wang, M. Wilson, P. K. Wolber, L. Zhang, S. Amur, W. Bao, C. C. Barbacioru, A. B. Lucas, V. Bertholet, C. Boysen, B. Bromley, D. Brown, A. Brunner, R. Canales, X. M. Cao, T. A. Cebula, J. J. Chen, J. Cheng, T. M. Chu, E. Chudin, J. Corson, J. C. Corton, L. J. Croner, C. Davies, T. S. Davison, G. Delenstarr, X. Deng, D. Dorris, A. C. Eklund, X. H. Fan, H. Fang, S. Fulmer-Smentek, J. C. Fuscoe, K. Gallagher, W. Ge, L. Guo, X. Guo, J. Hager, P. K. Haje, J. Han, T. Han, H. C. Harbottle, S. C. Harris, E. Hatchwell, C. A. Hauser, S. Hester, H. Hong, P. Hurban, S. A. Jackson, H. Ji, C. R. Knight, W. P. Kuo, J. E. LeClerc, S. Levy, Q. Z. Li, C. Liu, Y. Liu, M. J. Lombardi, Y. Ma, S. R. Magnuson, B. Maqsodi, T. McDaniel, N. Mei, O. Myklebost, B. Ning, N. Novoradovskaya, M. S. Orr, T. W. Osborn, A. Papallo, T. A. Patterson, R. G. Perkins, E. H. Peters, R. Peterson, et al. (2006) The MicroArray Quality Control (MAQC) project shows inter- and intraplatform reproducibility of gene expression measurements. *Nat Biotechnol,* 24**,** 1151-61.

Shimada, M., I. Hernandez-Gonzalez, I. Gonzalez-Robayna & J. S. Richards (2006) Paracrine and autocrine regulation of epidermal growth factor-like factors in cumulus oocyte complexes and granulosa cells: key roles for prostaglandin synthase 2 and progesterone receptor. *Mol Endocrinol,* 20**,** 1352-65.

Shuhaibar, L. C., J. R. Egbert, R. P. Norris, P. D. Lampe, V. O. Nikolaev, M. Thunemann, L. Wen, R. Feil & L. A. Jaffe (2015) Intercellular signaling via cyclic GMP diffusion through gap junctions restarts meiosis in mouse ovarian follicles. *Proc Natl Acad Sci U S A*.

Silva, P. J., J. L. Juengel, M. K. Rollyson & G. D. Niswender (2000) Prostaglandin metabolism in the ovine corpus luteum: catabolism of prostaglandin F(2alpha) (PGF(2alpha)) coincides with resistance of the corpus luteum to PGF(2alpha). *Biol Reprod,* 63**,** 1229-36.

Simon, A. M., D. A. Goodenough, E. Li & D. L. Paul (1997) Female infertility in mice lacking connexin 37. *Nature,* 385**,** 525-9.

Simopoulos, A. P. (2002) The importance of the ratio of omega-6/omega-3 essential fatty acids. *Biomed Pharmacother,* 56**,** 365-79.

Skarzynski, D. J., G. Ferreira-Dias & K. Okuda (2008) Regulation of luteal function and corpus luteum regression in cows: hormonal control, immune mechanisms and intercellular communication. *Reprod Domest Anim,* 43 Suppl 2**,** 57-65.

Skinner, M. K. (2005) Regulation of primordial follicle assembly and development. *Hum Reprod Update,* 11**,** 461-71.

Smith, S. (1994) The animal fatty acid synthase: one gene, one polypeptide, seven enzymes. *FASEB J,* 8**,** 1248-59.

Smuc, T. & T. L. Rizner (2009) Expression of 17beta-hydroxysteroid dehydrogenases and other estrogen-metabolizing enzymes in different cancer cell lines. *Chem Biol Interact,* 178**,** 228-33.

So, W. K., Q. Fan, M. T. Lau, X. Qiu, J. C. Cheng & P. C. Leung (2014) Amphiregulin induces human ovarian cancer cell invasion by down-regulating E-cadherin expression. *FEBS Lett,* 588**,** 3998-4007.

Song, D., G. Liu, V. Luu-The, D. Zhao, L. Wang, H. Zhang, G. Xueling, S. Li, L. Désy, F. Labrie & G. Pelletier (2006) Expression of aromatase and 17beta-hydroxysteroid dehydrogenase types 1, 7 and 12 in breast cancer. An immunocytochemical study. *J Steroid Biochem Mol Biol,* 101**,** 136-44.

Su, Y. Q., X. Wu, M. J. O'Brien, F. L. Pendola, J. N. Denegre, M. M. Matzuk & J. J. Eppig (2004) Synergistic roles of BMP15 and GDF9 in the development and function of the oocyte-cumulus cell complex in mice: genetic evidence for an oocyte-granulosa cell regulatory loop. *Dev Biol,* 276**,** 64-73.

Sugimoto, Y. & S. Narumiya (2007) Prostaglandin E receptors. *J Biol Chem,* 282**,** 11613-7.

Sugimoto, Y., A. Yamasaki, E. Segi, K. Tsuboi, Y. Aze, T. Nishimura, H. Oida, N. Yoshida, T. Tanaka, M. Katsuyama, K. Hasumoto, T. Murata, M. Hirata, F. Ushikubi, M. Negishi, A. Ichikawa & S. Narumiya (1997) Failure of parturition in mice lacking the prostaglandin F receptor. *Science,* 277**,** 681-3.

Szajnik, M., M. J. Szczepanski, E. Elishaev, C. Visus, D. Lenzner, M. Zabel, M. Glura, A. B. DeLeo & T. L. Whiteside (2012) 17β Hydroxysteroid dehydrogenase type 12 (HSD17B12) is a marker of poor prognosis in ovarian carcinoma. *Gynecol Oncol,* 127**,** 587-94.

Tajima, K., M. Orisaka, T. Mori & F. Kotsuji (2007) Ovarian theca cells in follicular function. *Reprod Biomed Online,* 15**,** 591-609.

Takahashi, T., J. D. Morrow, H. Wang & S. K. Dey (2006) Cyclooxygenase-2-derived prostaglandin E(2) directs oocyte maturation by differentially influencing multiple signaling pathways. *J Biol Chem,* 281**,** 37117-29.

Theveneau, E. & R. Mayor (2010) Integrating chemotaxis and contact-inhibition during collective cell migration: Small GTPases at work. *Small GTPases,* 1**,** 113-117.

--- (2012) Neural crest delamination and migration: from epithelium-to-mesenchyme transition to collective cell migration. *Dev Biol,* 366**,** 34-54.

Tilley, S. L., L. P. Audoly, E. H. Hicks, H. S. Kim, P. J. Flannery, T. M. Coffman & B. H. Koller (1999) Reproductive failure and reduced blood pressure in mice lacking the EP2 prostaglandin E2 receptor. *J Clin Invest,* 103**,** 1539-45.

Tomikawa, J., Y. Uenoyama, M. Ozawa, T. Fukanuma, K. Takase, T. Goto, H. Abe, N. Ieda, S. Minabe, C. Deura, N. Inoue, M. Sanbo, K. Tomita, M. Hirabayashi, S. Tanaka, T. Imamura, H. Okamura, K. Maeda & H. Tsukamura (2012) Epigenetic regulation of Kiss1 gene expression mediating estrogen-positive feedback action in the mouse brain. *Proc Natl Acad Sci U S A,* 109**,** E1294-301.

Uefuji, K., T. Ichikura & H. Mochizuki (2001) Expression of cyclooxygenase-2 in human gastric adenomas and adenocarcinomas. *J Surg Oncol,* 76**,** 26-30.

Uhlenhaut, N. H. & M. Treier (2011) Forkhead transcription factors in ovarian function. *Reproduction,* 142**,** 489-95.

Unterwurzacher, I., T. Koal, G. K. Bonn, K. M. Weinberger & S. L. Ramsay (2008) Rapid sample preparation and simultaneous quantitation of prostaglandins and lipoxygenase derived fatty acid metabolites by liquid chromatography-mass spectrometry from small sample volumes. *Clin Chem Lab Med,* 46**,** 1589-97.

Ushikubi, F., E. Segi, Y. Sugimoto, T. Murata, T. Matsuoka, T. Kobayashi, H. Hizaki, K. Tuboi, M. Katsuyama, A. Ichikawa, T. Tanaka, N. Yoshida & S. Narumiya (1998) Impaired febrile response in mice lacking the prostaglandin E receptor subtype EP3. *Nature,* 395**,** 281-4.

Vaccari, S., K. Horner, L. M. Mehlmann & M. Conti (2008) Generation of mouse oocytes defective in cAMP synthesis and degradation: endogenous cyclic AMP is essential for meiotic arrest. *Dev Biol,* 316**,** 124-34.

Vaccari, S., J. L. Weeks, M. Hsieh, F. S. Menniti & M. Conti (2009) Cyclic GMP signaling is involved in the luteinizing hormone-dependent meiotic maturation of mouse oocytes. *Biol Reprod,* 81**,** 595-604.

van Casteren, J. I., W. G. Schoonen & H. J. Kloosterboer (2000) Development of time-resolved immunofluorometric assays for rat follicle-stimulating hormone and luteinizing hormone and application on sera of cycling rats. *Biol Reprod,* 62**,** 886-94.

Wang, Y., D. Botolin, J. Xu, B. Christian, E. Mitchell, B. Jayaprakasam, M. G. Nair, M. Nair, J. M. Peters, J. V. Busik, J. Busik, L. K. Olson & D. B. Jump (2006) Regulation of hepatic fatty acid elongase and desaturase expression in diabetes and obesity. *J Lipid Res,* 47**,** 2028-41.

Wang, Z. (2005) The role of COX-2 in oral cancer development, and chemoprevention/ treatment of oral cancer by selective COX-2 inhibitors. *Curr Pharm Des,* 11**,** 1771-7.

Wide, L. & K. Eriksson (2013) Dynamic changes in glycosylation and glycan composition of serum FSH and LH during natural ovarian stimulation. *Ups J Med Sci,* 118**,** 153-64.

Wiltbank, M. C., C. J. Belfiore & G. D. Niswender (1993) Steroidogenic enzyme activity after acute activation of protein kinase (PK) A and PKC in ovine small and large luteal cells. *Mol Cell Endocrinol,* 97**,** 1-7.

Wiltbank, M. C., M. G. Diskin, J. A. Flores & G. D. Niswender (1990) Regulation of the corpus luteum by protein kinase C. II. Inhibition of lipoprotein-stimulated steroidogenesis by prostaglandin F2 alpha. *Biol Reprod,* 42**,** 239-45.

Witkowski, A., A. K. Joshi & S. Smith (2002) Mechanism of the beta-ketoacyl synthase reaction catalyzed by the animal fatty acid synthase. *Biochemistry,* 41**,** 10877-87.

Xing, H., D. Weng, G. Chen, W. Tao, T. Zhu, X. Yang, L. Meng, S. Wang, Y. Lu & D. Ma (2008) Activation of fibronectin/PI-3K/Akt2 leads to chemoresistance to docetaxel by regulating survivin protein expression in ovarian and breast cancer cells. *Cancer Lett,* 261**,** 108-19.

Xu, J. & T. Gridley (2013) Notch2 is required in somatic cells for breakdown of ovarian germ-cell nests and formation of primordial follicles. *BMC Biol,* 11**,** 13.

Yan, C., P. Wang, J. DeMayo, F. J. DeMayo, J. A. Elvin, C. Carino, S. V. Prasad, S. S. Skinner, B. S. Dunbar, J. L. Dube, A. J. Celeste & M. M. Matzuk (2001) Synergistic roles of bone morphogenetic protein 15 and growth differentiation factor 9 in ovarian function. *Mol Endocrinol,* 15**,** 854-66.

Yeh, C. M., Y. C. Liu, C. J. Chang, S. L. Lai, C. D. Hsiao & S. J. Lee (2011) Ptenb mediates gastrulation cell movements via Cdc42/AKT1 in zebrafish. *PLoS One,* 6**,** e18702.

Young, J. M. & A. S. McNeilly (2010) Theca: the forgotten cell of the ovarian follicle. *Reproduction,* 140**,** 489-504.

Annales Universitatis Turkuensis

Turun yliopisto
University of Turku

Painosalama Oy, Turku, Finland 2018

ISBN 978-951-29-7109-1 (PRINT)
ISBN 978-951-29-7110-7 (PDF)
ISSN 0355-9483 (PRINT) | ISSN 2343-3213 (PDF)